Alzheimer's
Research & Therapy

RESEARCH

Open Access

A single-domain antibody detects and neutralises toxic $A\beta_{42}$ oligomers in the Alzheimer's disease CSF

Alessandra Bigi[1†], Liliana Napolitano[1†], Devkee M. Vadukul[2], Fabrizio Chiti[1], Cristina Cecchi[1], Francesco A. Aprile[2,3] and Roberta Cascella[1*]

Abstract

Background Amyloid-β_{42} ($A\beta_{42}$) aggregation consists of a complex chain of nucleation events producing soluble oligomeric intermediates, which are considered the major neurotoxic agents in Alzheimer's disease (AD). Cerebral lesions in the brain of AD patients start to develop 20 years before symptom onset; however, no preventive strategies, effective treatments, or specific and sensitive diagnostic tests to identify people with early-stage AD are currently available. In addition, the isolation and characterisation of neurotoxic $A\beta_{42}$ oligomers are particularly difficult because of their transient and heterogeneous nature. To overcome this challenge, a rationally designed method generated a single-domain antibody (sdAb), named DesAb-O, targeting $A\beta_{42}$ oligomers.

Methods We investigated the ability of DesAb-O to selectively detect preformed $A\beta_{42}$ oligomers both in vitro and in cultured neuronal cells, by using dot-blot, ELISA immunoassay and super-resolution STED microscopy, and to counteract the toxicity induced by the oligomers, monitoring their interaction with neuronal membrane and the resulting mitochondrial impairment. We then applied this approach to CSF samples (CSFs) from AD patients as compared to age-matched control subjects.

Results DesAb-O was found to selectively detect synthetic $A\beta_{42}$ oligomers both in vitro and in cultured cells, and to neutralise their associated neuronal dysfunction. DesAb-O can also identify $A\beta_{42}$ oligomers present in the CSFs of AD patients with respect to healthy individuals, and completely prevent cell dysfunction induced by the administration of CSFs to neuronal cells.

Conclusions Taken together, our data indicate a promising method for the improvement of an early diagnosis of AD and for the generation of novel therapeutic approaches based on sdAbs for the treatment of AD and other devastating neurodegenerative conditions.

Keywords Nanobodies, Conformation-sensitive antibodies, Amyloid β peptide, Protein misfolding, Early diagnosis, Biofluids, $A\beta_{42}$-targeting therapy, Neurodegenerative diseases

[†]Alessandra Bigi and Liliana Napolitano contributed equally to this work.

*Correspondence:
Roberta Cascella
roberta.cascella@unifi.it
Full list of author information is available at the end of the article

Background

Alzheimer's disease (AD) is the most prevalent neurodegenerative disorder affecting ca. 60–70% of 55 million people worldwide suffering with some form of dementia (Alzheimer's association, 2023). It is characterised by the presence of extracellular amyloid-β (Aβ) plaques and intracellular tau neurofibrillary tangles in specific vulnerable populations of neurons, thus leading to their death [1–3]. In the last decades, small oligomers of the 42-residue form of Aβ ($Aβ_{42}$), formed early during the aggregation process or released from mature fibrils, have acquired increasing importance as primary toxic species in AD pathogenesis [4–7]. Indeed, elevated oligomer levels in the brain are associated with pathology [8] and correlate better with the degree of dementia as compared to mature fibrils [9]. Moreover, in some transgenic mouse models overexpressing mutant amyloid precursor protein (APP), synaptic alteration and cognitive impairment precede amyloid plaque formation, but occur after Aβ levels start to rise steadily [10, 11].

In the past few years, considerable effort has been made to identify the structural determinants of oligomer neurotoxicity, including oligomer size and hydrophobic exposure [12, 13], that are responsible for their ability to trigger several toxic pathways, ultimately leading to neuronal death [5, 13, 14]. Notably, soluble Aβ oligomers have been recently identified within the cerebrospinal fluid (CSF) of mild cognitive impaired (MCI) and AD [15–17] patients. In particular, conformation-sensitive antibodies (Abs) directed against well-defined forms of $Aβ_{42}$ oligomers, have detected oligomers in AD brains that were absent in age-matched healthy individuals [18–21]. The aggregate distribution varies in terms of structure, size and shape but also toxicity along AD progression [17], so that an efficient method to distinguish and quantify these species could serve diagnostic and therapeutic purposes. Indeed, the lack of specific and sensitive diagnostic tests to identify people with early-stage AD to be included in clinical trials is among the main reasons for many notable trial failures, considering that cerebral lesions occur 20 years before symptom onset [22–25].

Over the past 25 years, several monoclonal Abs (mAbs) have been engineered to bind and eliminate Aβ [26] from the brain of AD patients and are currently under investigation in clinical trials. Although some Abs, such as Aducanumab (Aduhelm™), initially appeared to be able to eliminate parenchymal amyloid [27], they have so far failed to change cognition in subjects with MCI and AD [9]. More recently, in 2023, the FDA approved another mAb, Lecanemab (Leqembi™), which slows down cognitive decline in AD [28]. Both mAbs are recommended for the early stages of AD but, unfortunately, they can only slow down AD decline without stopping it completely or reverting it [28–30].

The capture of small soluble protein aggregates to reduce their toxicity could be an important therapeutic strategy for AD. In this context, nanobodies or single-domain Abs (sdAbs) could constitute a real breakthrough for the treatment of AD [31], but also for early diagnosis of AD. sdAbs, firstly discovered in 1993, are recombinant, antigen-specific, variable fragments of camelid heavy chain-only Abs (VHH) [32]. As classical Abs, they retain high target specificity and affinity, but their small size makes them highly stable, soluble, able to access clefts and hidden epitopes and to be functionally expressed as intrabodies [33]. Moreover, their low immunogenic potential and inherent toxicity make them great tools for basic research and potential candidates for both diagnostic and therapeutic applications [31, 33].

Previously published works [34, 35] demonstrated that targeting the region 29 to 36 of $Aβ_{42}$ with rationally designed Abs, also called DesAbs [36, 37], can inhibit the peptide's secondary nucleation. Among these DesAbs, DesAb-O was found to preferentially bind to $Aβ_{42}$ oligomers rather than its monomeric and fibrillar forms, as this region is likely to be solvent-exposed when the peptide is oligomeric, before becoming buried in amyloid fibrils [35].

In this study, we investigated the ability of DesAb-O to selectively detect preformed $Aβ_{42}$ oligomers both in vitro and in cultured cells and to counteract their neurotoxicity, taking advantage of commercially available conformation-sensitive Abs, as controls. By using dot-blot, ELISA immunoassay and stimulated emission depletion (STED) microscopy, we demonstrated the high ability of DesAb-O to identify $Aβ_{42}$ oligomers rather than monomers and fibrils. Moreover, DesAb-O was found to significantly inhibit oligomer binding to neuronal membranes, restoring mitochondrial functionality. We then applied this approach to CSF samples (CSFs) from AD patients as compared to healthy individuals. We demonstrated the presence of well-resolved $Aβ_{42}$ oligomeric species in the CSF of AD patients, clearly detected by DesAb-O. Moreover, the administration of AD CSFs to cultured neuronal cells caused detrimental effects that were completely abolished by the pre-incubation with DesAb-O.

These findings strongly suggest that the use of sdAbs to detect soluble toxic species in biofluids offers a promising way for the improvement of an early diagnosis of AD. Our study also reveals a powerful ability of DesAb-O to prevent $Aβ_{42}$ neurotoxicity, contributing to the generation of

novel therapeutic approaches based on sdAbs for AD and other neurodegenerative diseases.

Methods

Preparation of $A\beta_{42}$ aggregates

$A\beta_{42}$ conformers were prepared as previously reported [38–40]. Briefly, the lyophilised peptide (Bachem) was dissolved in 100% hexafluoro-2-isopropanol (HFIP) to 1 mM and the solvent was then evaporated under nitrogen. To obtain $A\beta_{42}$ oligomers, the peptide was resuspended in 50 mM NaOH at 1 mg/ml and diluted in PBS to a final concentration of 25 µM. Then, the sample was centrifuged at 22,000 *g* for 30 min, the pellet discarded and the supernatant incubated at 25 °C without agitation for 1 day to obtain A + oligomers or for 4 days to obtain A − oligomers [40]. F1 were obtained, with the same procedure, at a final concentration of 50 µM after 1 day of incubation [40]. Amyloid β-derived diffusible ligands (ADDLs) were obtained by dissolving an aliquot of the peptide in anhydrous dimethyl sulfoxide (DMSO) to 5 mM and then diluting in ice-cold F-12 medium to a final concentration of 100 µM. This solution was incubated at 4 °C for 1 day and then centrifuged at 14,000 × *g* for 10 min [38]. Finally, F2 were prepared by dissolving the peptide in DMSO to 5 mM and then diluting it in 10 mM HCl to a final concentration of 100 µM. The sample was incubated at 37 °C without agitation for 1 day [39].

CSF samples

CSF samples (CSFs) from human aged controls ($n = 4$) or AD patients ($n = 9$) were obtained from BioIVT. Each CSF was received in 0.5–1 ml aliquot and stored at − 80 °C. Samples were centrifuged at 4000 *g* for 10 min at 4 °C, obtaining a pale pellet that was separated from the supernatant. The supernatant was then analysed; protein concentration in these samples was determined by the Bradford colorimetric method [41].

DesAb-O and DesAb18–24 purification

DesAb-O and DesAb18–24 were purified as previously described [34]. Briefly, DesAb-O and DesAb18–24 were expressed in *E.Coli* Origami™ (DE3) pLysS cells (Merck Millipore), and grown for at least 15 h at 30 °C in Overnight Express Instant TB Medium (Merck Millipore) supplemented with 100 µg/ml ampicillin. Cells were collected by centrifugation, resuspended in PBS (8 mM Na_2HPO_4, 15 mM KH_2PO_4, 137 mM NaCL, and 3 mM KCl, pH 7.3) with an EDTA-Free Complete Protease Inhibitor Cocktail tablet (Roche). Cells were lysed by sonication and cellular debris was removed by centrifugation. The supernatant was applied to a HisTrap HP 5 ml column (Cytiva) that has been pre-equilibrated with PBS supplemented with 15 mM imidazole. The column was then washed with several column volumes of PBS supplemented with 15 mM imidazole after which the Ab was eluted in PBS with 300 mM imidazole. The sample was then dialysed against PBS overnight at 4 °C to remove imidazole, after which it was applied to a HiLoad Superdex 75 16/600 pg (Cytiva) column for size exclusion chromatography. Protein concentration was determined by measuring the absorbance at 280 nm and using the molecular coefficient of DesAb-O or DesAb18–24.

Dot-blot analysis

Dot-blot analysis was performed by spotting 2.0 µl (corresponding to 0.1 µg) of each $A\beta_{42}$ conformer onto a nitrocellulose membrane. After 30 min blocking (1.0% bovine serum albumin, BSA, in TBS/TWEEN 0.1%), $A\beta_{42}$ species were probed with 2 µM DesAb-O or with 1:15.000 diluted human monoclonal anti-ADDLs (19.3) Ab (Creative Biolabs), or with 1:1000 diluted rabbit polyclonal anti-oligomer (A11) Ab (Thermo Fisher Scientific), or with 1:1000 diluted rabbit polyclonal anti-amyloid fibrils (OC) Ab (Sigma-Aldrich), or with 1:1000 diluted mouse monoclonal anti-Aβ (6E10) Ab (Biolegend Way) and then with 1:2000 diluted goat anti-6X His tag (Abcam), or goat anti-human (Sigma-Aldrich), or goat anti-rabbit (Abcam) or rabbit anti-mouse (Abcam) horseradish peroxidase (HRP) conjugated secondary Abs. In another set of experiments, decreasing quantities (0.1, 0.05, 0.0025, 0.001 and 0.005 µg) of $A\beta_{42}$ aggregates were spotted onto the nitrocellulose membrane, and then probed with DesAb-O and 19.3 Abs, as described above. The immunolabelled dots were detected using a SuperSignalWest Dura (Pierce) ImageQuant™ TL software (GE Healthcare UK Limited version 8.2).

In a set of experiments, sandwich dot-blot was performed. Briefly, 2 µl of 6E10 and DesAb-O Abs (0.01 mg/ml and 10 µM, respectively) were spotted onto nitrocellulose membranes. After 20 min, the blots were blocked in TBS-Tween-20 0.2% and 2.5% BSA IgG free for 40 min. The membranes were incubated with different $A\beta_{42}$ species at 0.01 mg/ml (monomeric $A\beta_{42}$, A + oligomers, F1) or with the CSFs of AD patients and control subjects at 0.1 mg/ml. Then, the membranes were probed with 1:1000 diluted 6E10 Ab overnight at 4 °C under constant shaking. The following day, the membranes were washed three times in TBS-Tween-20 0.2% and incubated with 1:3000 diluted rabbit anti-mouse HRP-conjugated secondary Ab for 1 h. After three additional washes, the immunolabelled dots were detected as reported above.

ELISA assay

For indirect ELISA assay, increasing concentrations (0, 1, 5, and 10 µM, monomer equivalents) of each $A\beta_{42}$

conformer, prepared as reported above, were immobilised on a 96-well Maxisorp ELISA plate (Nunc) under quiescent conditions for 1 h at room temperature (RT). The plate was then washed three times with 20 mM Tris, pH 7.4, and 100 mM NaCl and incubated in 20 mM Tris, pH 7.4, 100 mM NaCl, and 5% BSA under constant shaking overnight at 4 °C. The day after the plate was washed six times with 20 mM Tris, pH 7.4, and 100 mM NaCl and then incubated with 40 µL solutions of 2.0 µM DesAb-O, or with 1:20,000 diluted 19.3 Ab, or with 1:8000 diluted 6E10 Ab, under constant shaking for 1 h at RT. The plate was then washed six times with 20 mM Tris, pH 7.4, and 100 mM NaCl and incubated with 1:2000 diluted goat anti-6X His tag, 1:5000 diluted goat anti-human and 1:4000 rabbit anti-mouse HRP-conjugated secondary Abs, in 20 mM Tris, pH 7.4, 100 mM NaCl, and 5% BSA under shaking for 1 h at RT. Finally, the plate was washed three times with 20 mM Tris, pH 7.4, and 100 mM NaCl, then twice with 20 mM Tris, pH 7.4, 100 mM NaCl, and 0.02% Tween-20, and again three times with 20 mM Tris, pH 7.4, and 100 mM NaCl. Finally, the amount of bound Abs was quantified by using 1-Step Ultra TMB-ELISA Substrate Solution (Thermo Fisher Scientific), according to the manufacturer's instructions, and the reaction was stopped by adding 40 µl of H_2SO_4. Then, the absorbance was measured at 450 nm by means of a CLARIOstar plate reader (BMG Labtech).

For sandwich ELISA assay, 1 µM DesAb-O or 0.5 µM DesAb18–24 Abs were immobilised on a 96-well Maxisorp ELISA plate under quiescent conditions for 1 h at RT. After three washes in PBS, the plate was blocked with 5% BSA IgG free overnight at 4 °C under constant shaking. The day after, the plate was washed six times in PBS and different $A\beta_{42}$ species (M, A + oligomers, F1 at decreasing concentrations (4500, 2250, 450, 45, 4.5 and 2.25 pg/ml for DesAb-O and $4500{\cdot}10^3$ pg/ml, 4500 pg/ml and 4.5 pg/ml for DesAb18–24) and the CSFs of AD patients ($n=9$) and control subjects ($n=4$) at 0.25 mg/ml were loaded into the plate overnight at 4 °C under constant shaking. In the DesAb-O plate, we loaded 4500 pg/ml of monomeric αSynuclein (αSyn) as negative control. The following day after six additional washes in PBS, the plate was incubated with 1:4000 6E10 Ab for 2 h at RT with no shaking, while αSyn was incubated with 1:4000 diluted mouse monoclonal anti-αSyn (211) Ab (Santa Cruz Biotechnology). The plate was washed six times in PBS-Tween-20 0.2% and incubated with 1:5000 rabbit anti-mouse HRP- conjugated secondary Ab for 1 h at RT. The plate was then washed six additional times in PBS-Tween-20 0.2% and the amount of $A\beta_{42}$ species bound was quantified as reported above.

Cell cultures

Authenticated human SH-SY5Y neuroblastoma cells were purchased from A.T.C.C. and cultured in Dulbecco's modified Eagle's medium (DMEM), F-12 Ham with 25 mM 4-(2-Hydroxyethyl) piperazine-1-ethanesulfonic acid (HEPES) and $NaHCO_3$ (1:1) supplemented with 10% foetal bovine serum (FBS), 1.0 mM glutamine and 1.0% penicillin and streptomycin solution (Sigma-Aldrich). Cells were maintained in a 5.0% CO_2 humidified atmosphere at 37° C and grown until 80% confluence for a maximum of 20 passages, and tested to ensure that they were free form mycoplasma contamination [42]. Primary rat cortical neurons (Thermo Fisher Scientific) were plated in 12-well plate containing glass coverslips and maintained in neuronal basal plus medium (Thermo Fisher Scientific) supplemented with GlutaMAX (Gibco, Thermo Fisher Scientific) at the concentration of 0.5 mM and 2% (v/v) B-27 serum-free complement (Gibco, Thermo Fisher Scientific), in a 5% CO_2 humidified atmosphere at 37 °C. Every 2 days the medium was partially replaced with fresh one. The experiments were performed 14 days after plating [43].

STED microscopy

$A\beta_{42}$ assemblies were added to the culture medium of SH-SY5Y cells seeded on glass coverslips for 1 h at 3 µM (monomer equivalents). After incubation, the cells were washed with PBS, the plasma membranes were counterstained with 0.01 mg/ml tetramethylrhodamine-conjugated wheat germ agglutinin (WGA;Thermo Fisher Scientific) [44] for 15 min at 37 °C and cells were then fixed with 2.0% (w/v) paraformaldehyde for 10 min at RT. After washing with PBS, the plasma membranes were permeabilised with a 3.0% (v/v) glycerol solution for 10 min at RT. $A\beta_{42}$ species were then detected with 4 µM DesAb-O and 1:800 diluted FITC anti-6X tag secondary Abs (Abcam), or with 1:250 diluted human monoclonal (19.3) anti-oligomer Ab and 1:1000 diluted Alexa Fluor 488-conjugated anti-human secondary Ab (Thermo Fisher Scientific), or with 1:400 diluted A11 Ab, or with 1:800 diluted OC Ab, or with 1:400 diluted 6E10 Ab and 1:500 diluted Alexa Fluor 514-conjugated anti-rabbit or anti-mouse secondary Abs (Thermo Fisher Scientific). STED xyz images (i.e., *z*-stacks acquired along 3 directions: *x*, *y*, and *z* axes) were acquired as previously reported [44]. In a set of experiments, SH-SY5Y cells seeded on glass coverslips were experienced for 24 h with ADDLs at 3.0 µM (monomer equivalents) or CSFs from AD patients or controls ($n=4$ for both AD and control CSFs) diluted 1:1 with cellular medium. In another set of experiments, primary rat cortical neurons were treated with CSFs from AD patients or controls ($n=4$ for both AD and control CSFs) diluted 1:1 with cellular medium.

After the incubation, the cells were counterstained and analysed by STED microscopy as reported above. In another set of experiments, A + oligomers, F1 and a mixture containing both $A\beta_{42}$ species (1:1 molar ratio) were incubated on a glass coverslip at 25 µM in PBS without cells while the CSFs ($n = 9$ and $n = 4$ for AD and controls, respectively) were spotted at a concentration of 0.5 mg/ml. After 30 min of incubation, the samples were blocked in Casein 1X with TBS-Tween-20 0.2% for 30 min. Once washed with TBS-Tween-20 0.2%, $A\beta_{42}$ species and the CSFs were detected with 1:800 diluted 6E10, 2.0 µM DesAb-O or 4 µM DesAb18–24 Ab for 1 h and then with 1:500 diluted Alexa Fluor 514-conjugated anti-mouse secondary Abs or with 1:500 FITC anti-6X tag secondary Abs. The acquisition was performed as reported above.

Confocal microscopy analysis of $A\beta_{42}$ aggregates bound to neuronal membranes

SH-SY5Y cells were seeded on glass coverslips and then treated for 15 min with A + oligomers or ADDLs at a concentration of 3.0 µM (monomer equivalents), in the absence or presence of a pre-incubation with increasing molar ratios (1:0.1, 1:0.25, 1:0.5 and 1:1, monomer equivalents) between Abs and $A\beta_{42}$ species. After incubation, the cells were washed with PBS and the plasma membranes were counterstained for 15 min with 5.0 µg mL^{-1} Alexa Fluor 633-conjugated WGA (Thermo Fisher Scientific) [6]. Cells were fixed in 2.0% (w/v) paraformaldehyde for 10 min at RT and $A\beta_{42}$ assemblies were detected with 1:800 diluted 6E10 Ab and then 1:1000 diluted Alexa Fluor 488-conjugated anti-mouse secondary Ab (Thermo Fisher Scientific). To detect only the oligomers bound to the cell surface, the cellular membrane was not permeabilised, thus preventing Ab internalisation. Fluorescence emission was detected after double excitation at 633 and 488 nm by a TCS SP8 scanning confocal microscopy system (Leica Microsystems), as previously described [45]). The degree of colocalisation of $A\beta_{42}$ aggregates with the cell membranes was estimated in regions of interest in 30–32 cells, via the use of ImageJ software (NIH) and JACOP plugin (http://rsb.info.nih.gov) (Rasband WR).

MTT reduction assay

The cytotoxicity of the different $A\beta_{42}$ aggregates was assessed in SH-SY5Y cells seeded in 96-well plates by the 3-(4,5-dimethylthiazol-2-yl)-2,5-diphenyltetrazolium bromide (MTT) assay [46, 47]. Briefly, $A\beta_{42}$ species (monomer, A + and A − oligomers, ADDLs, F1 and F2) at a concentration of 3.0 µM (monomer equivalents) were added to the culture medium of SH-SY5Y cells for 24 h following or not a pre-incubation under shaking with equimolar concentrations of DesAb-O, 19.3, A11 or OC Abs. After treatment, the culture medium was removed, cells were washed with PBS and the MTT assay was assessed as previously reported [7]. Cell viability was expressed as the percentage of MTT reduction in treated cells as compared to those untreated (taken as 100%), or to those treated with $A\beta_{42}$ species in the absence of Abs.

In a set of experiments, CSFs ($n = 4$ for AD as well as controls) were added to the culture medium of SH-SY5Y cells for 24 h following a 1 h pre-incubation in the absence or presence of DesAb-O at 3 µM at 37 °C under shaking conditions. Cells treated with ADDLs at 1 µM (monomer equivalents) were used as positive control. The analysis was performed as reported above.

Measurement of cytosolic free Ca^{2+} levels

The intracellular calcium levels were measured in SH-SY5Y cells as previously described [7, 48]. SH-SY5Y cells were treated for 5 h with the CSFs ($n = 4$ for AD as well for controls) in the absence or presence a 1 h pre-incubation with DesAb-O at 3 µM under shaking. At the end of the treatment, the cells were washed in PBS and loaded with 4.5 µM Fluo-4 AM (Thermo Fisher Scientific) for 10 min and cytosolic Ca^{2+} levels were detected after excitation at 488 nm by the TCS SP8 scanning confocal microscopy system as previously reported [7, 44]. Cells treated with ADDLs at 1 µM (monomer equivalents) were used as positive control. Images were then analysed using the ImageJ software, and the fluorescence intensities were expressed as the percentage of that measured in untreated cells, taken as 100%.

Measurements of calcein leakage

The intracellular calcein levels were measured in SH-SY5Y cells as previously described [44]. Briefly, the cells were washed in PBS and loaded with 0.5 µM Calcein-AM (Thermo Fisher Scientific) for 20 min at 37 °C. Then, they were washed with PBS and treated for 5 h with CSFs ($n = 4$ for both AD and control CSFs) in the absence or presence of a 1 h pre-incubation with DesAb-O at 3 µM under shaking. Cells treated with ADDLs at 1 µM (monomer equivalents) were used as positive control. After fixation in 2.0% buffered paraformaldehyde for 10 min at RT, fluorescence emission was detected after excitation at 488 nm by the TCS SP8 scanning confocal microscopy system as previously reported [44]. Images were then analysed as reported above.

Statistical analysis

Data were expressed as means ± standard deviation (S.D.), or as means ± standard error of mean (S.E.M). Comparisons between the different groups were performed by using the Student *t* test or the one-way ANOVA followed

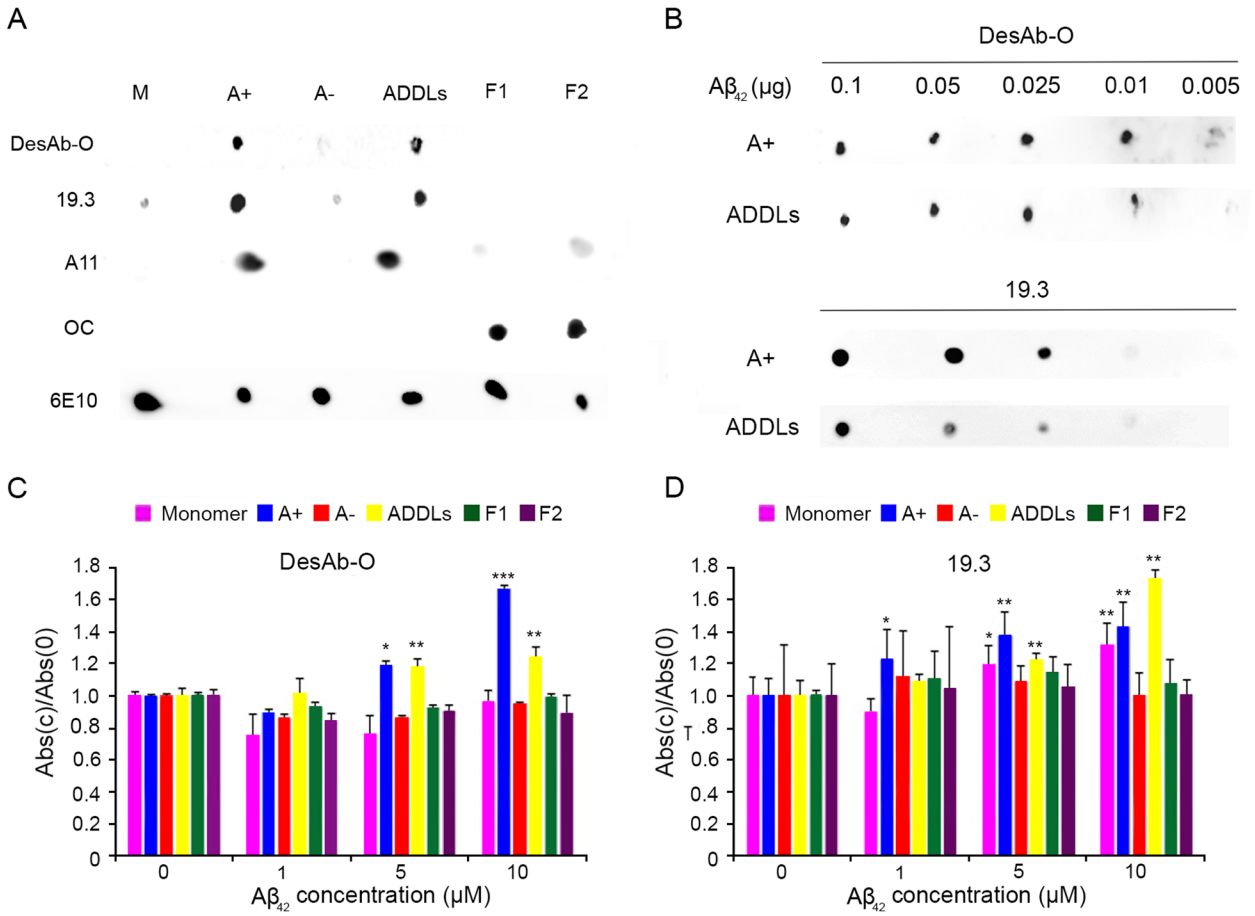

Fig. 1 DesAb-O selectively detects synthetic $A\beta_{42}$ oligomers in vitro. **A**,**B** Dot-blot analysis of $A\beta_{42}$ species. **A** Samples of monomeric $A\beta_{42}$ (M), oligomeric (A+, A−and ADDLs) and two types of fibrillar species (F1 from [40] and F2 from [39]) were deposited (2 µl/spot, corresponding to 0.1 µg) onto a nitrocellulose membrane and detected with the indicated Abs. **B** Samples of A+oligomers and ADDLs at various amounts (0.25, 0.10, 0.05, 0.025, 0.01, 0.005 µg) were probed with DesAb-O (top) and 19.3 (bottom) Abs. **C**,**D** ELISA measurements taken at increasing concentration of $A\beta_{42}$ species using DesAb-O (**C**) and 19.3 (**D**) Abs. Data were normalised for the corresponding average value at concentration 0 µM. Experimental errors are S.D. ($n=3$). Samples were analysed by Student *t* test relative to 0 µM (*$P<0.05$, **$P<0.01$ and ***$P<0.001$)

by Bonferroni's multiple-comparison test (GraphPad Prism 5.0 software). *P* values lower than 0.05, 0.01 and 0.001 were considered to be statistically significant (*), highly statistically significant (**) and very highly statistically significant (***), respectively.

Results

DesAb-O selectively detects synthetic $A\beta_{42}$ oligomers in vitro

We firstly evaluated the specificity of DesAb-O against different $A\beta_{42}$ conformers by dot-blot analysis. $A\beta_{42}$ conformers were assembled in vitro according to well-defined protocols. Thus, toxic A+and nontoxic A−oligomers [40], toxic $A\beta_{42}$ ADDLs [38] and two types of fibrils, namely F1 [40] and F2 [39] were formed and their identities were confirmed by routinely analysing them by atomic force microscopy (AFM) and dot-blots using their respective conformation-sensitive Abs, as previously reported [49]. The various $A\beta_{42}$ species were then deposited (2 µl, corresponding to 0.1 µg) onto a nitrocellulose membrane and detected with DesAb-O and, as a control, with the 19.3 Ab, specific for amyloid β-derived diffusible ligands (ADDLs) [16], A11 Ab, recognising toxic oligomers from various proteins, but not their monomeric or fibrillar conformations [18], and OC Ab, specifically raised against fibrillar aggregates [20].

DesAb-O was found to selectively target toxic A+oligomers and ADDLs, with a minor cross-reaction with nontoxic A−oligomers (Fig. 1A). As expected, each of the abovementioned control Abs bound to their targeted conformers according to previous reports [16, 18, 20, 40, 45]. Proper loading of each $A\beta_{42}$ species was confirmed by the sequence-specific 6E10 Ab which targets the N-terminus

of $A\beta_{42}$ [18, 20, 50, 51], that bound all the analysed $A\beta_{42}$ species, independently of their aggregation state (Fig. 1A).

We then assessed the sensitivity of DesAb-O by evaluating its ability to probe decreasing amounts of $A\beta_{42}$ conformers (0.10, 0.05, 0.025, 0.01 and 0.005 μg), previously deposited onto a nitrocellulose membrane (Fig. 1B). DesAb-O was found to detect A + oligomers and ADDLs down to 0.01 μg, which appeared more sensitive when compared to the control 19.3 Ab (Fig. 1B).

The reactivity of DesAb-O against $A\beta_{42}$ species was also quantified by performing an indirect ELISA assay. Briefly, we coated the wells of the ELISA plates with increasing concentrations of $A\beta_{42}$ conformers (0, 1, 5 and 10 μM, monomer equivalents). We then incubated the plates with DesAb-O and subsequently with the appropriate secondary Abs. Our results showed that DesAb-O clearly recognised toxic A + oligomers and ADDLs at 5 and 10 μM, with a specificity that increased with aggregate concentration (Fig. 1C), revealing no affinity for the monomeric or fibrillar forms even at high concentrations (Fig. 1C). The 19.3 Ab was also assessed for a relative comparison, revealing high affinity for A + oligomers and ADDLs, even at 1 μM for the former species, but showing a minor specificity for $A\beta_{42}$ monomers (Fig. 1D). As expected, the 6E10 Ab was found to detect all the analysed $A\beta_{42}$ conformers in a dose-dependent manner (Fig. S1), as the $A\beta_{42}$ N-terminus is solvent-exposed regardless of the aggregated state of the peptide [17]. Overall, dot-blot and ELISA results demonstrate the ability of DesAb-O to selectively discriminate $A\beta_{42}$ conformers, in agreement with previously established work [34, 35]. Moreover, the affinity of DesAb-O against $A\beta_{42}$ oligomers and its selectivity for the oligomeric species with respect to the monomers and fibrils do not seem to be any worse than those observed with commercially available Abs, providing the platform for further applications.

DesAb-O detects synthetic $A\beta_{42}$ oligomers bound to neuronal membrane and internalised into the cytosol

To analyse whether or not the ability of DesAb-O to selectively detect $A\beta_{42}$ oligomers in vitro is also reflected in cultured cells, human neuroblastoma SH-SY5Y cells were exposed for 1 h to different types of $A\beta_{42}$ species at 3.0 μM (monomer equivalents) and then the plasma membrane (red channel) and $A\beta_{42}$ aggregates (green channel) were counterstained and analysed by the super-resolution STED microscope [44] (Fig. 2). DesAb-O was found to detect toxic A + oligomers and ADDLs (Fig. 2A), showing an increase of the green fluorescent signal by 1362 ± 46% and 1010 ± 45%, respectively, with respect to the untreated cells, taken as 100% (Fig. 2B). In particular, by analysing different optical sections (apical, median and basal planes to the coverslip), DesAb-O can identify these oligomers bound to the neuronal membranes and penetrating into the cells (Fig. S2). Similar results were obtained with the 19.3 Ab (1010 ± 99% and 1235 ± 39%) and to a lower extent with the A11 one (680 ± 66% and 633 ± 97%) (Fig. 2A,B). The OC Ab specifically recognised both types of fibrillar conformers (F1 and F2), which appeared predominantly bound to the plasma membranes, and the green fluorescent signal increased by 557 ± 55% and 562 ± 57% for the former type of fibril [40] and the latter type of fibril [39], respectively (Fig. 2A,B). As expected, the sequence-specific 6E10 Ab detected both A + oligomers and ADDLs and F1 and F2 fibrils on neuronal cells (Fig. 2A,B). None of the Abs detected non-toxic A − oligomers that evoked a very low and undetectable fluorescent signal because they are known to weakly interact with neuronal membranes [40, 45, 49].

Overall, in our experimental conditions, DesAb-O selectively discriminated toxic $A\beta_{42}$ oligomers with respect to monomeric and fibrillar forms of the peptide, at least similarly to the other commercially available conformation-sensitive Abs, suggesting a very promising potential for the detection of harmful $A\beta_{42}$ species in biological fluids.

DesAb-O inhibits the interaction of $A\beta_{42}$ oligomers with neuronal membranes preventing mitochondrial dysfunction

We further evaluated whether DesAb-O was also able to capture $A\beta_{42}$ oligomers, preventing their detrimental effects on neuronal cells. To this purpose, A + oligomers and ADDLs were pre-incubated for 1 h with DesAb-O at increasing molar ratios between oligomers and Ab (from 1:0.1 to 1:1), and these solutions were then added to the cell culture medium of SH-SY5Y cells for 15 min. Unlike previous experiments, the oligomers were added to cultured cells only after pre-incubation with DesAb-O. To detect only the oligomers bound to the cell surface, the cellular membrane was not permeabilised at this stage, thus preventing antibody internalisation. The binding affinity of the aggregates for cellular membranes was assessed by confocal microscopy using the 6E10 Ab as a probe. Our results showed a strong colocalisation of $A\beta_{42}$ A + oligomers and ADDLs with the neuronal membranes in the absence of the pre-incubation with Ab (Fig. 3A), confirming previously reported data [45, 52, 53]. Notably, the binding of both types of $A\beta_{42}$ aggregates was significantly reduced in the presence of DesAb-O up to 1:0.1 molar ratio (by 40 ± 3% and 36 ± 2%, respectively) (Fig. 3A,C). The same analysis was performed with the A11 Ab, which was found to prevent the interaction of the oligomers with the membrane only at 1:1 molar ratio (by 44 ± 5% and 48 ± 7%, respectively) (Fig. 3B,D). These results again suggested a great affinity of DesAb-O for the

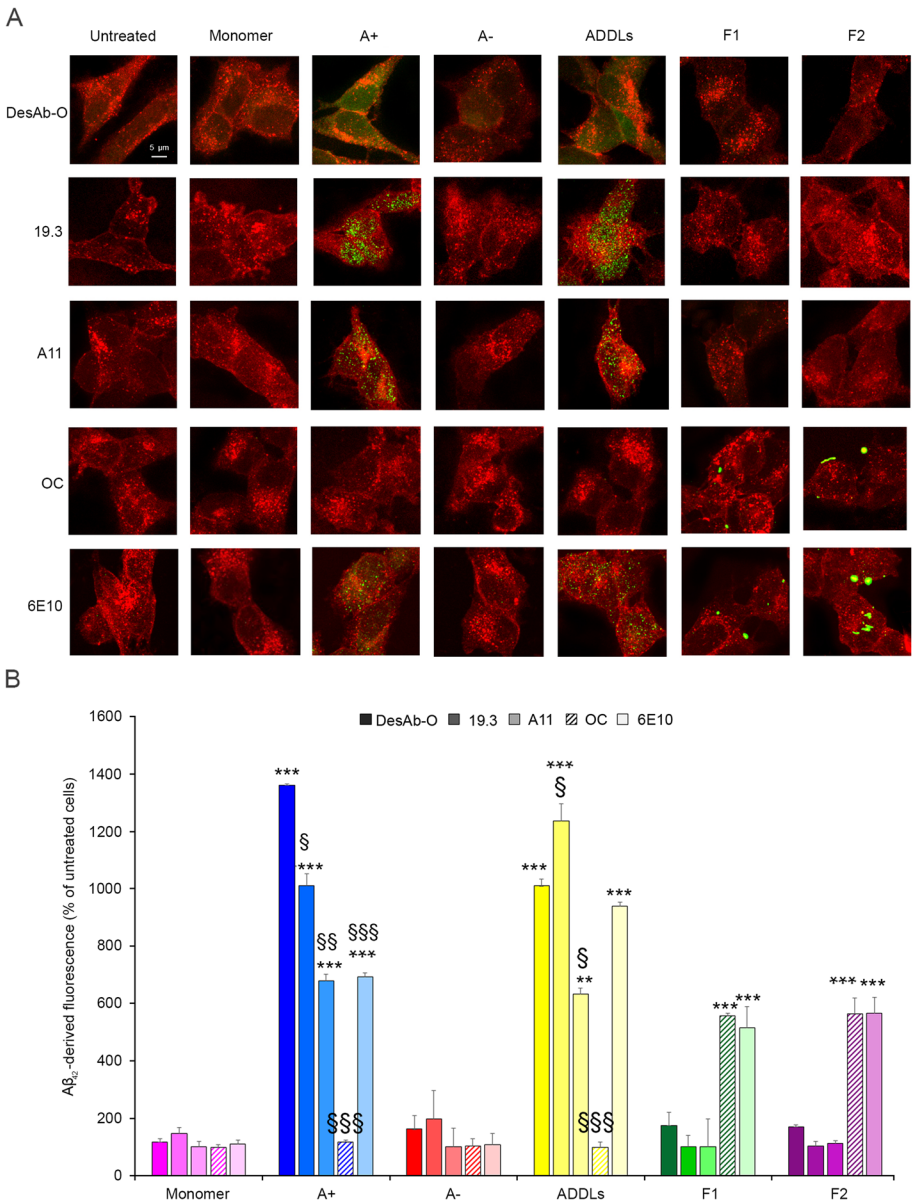

Fig. 2 DesAb-O detects synthetic $A\beta_{42}$ oligomers interacting with neuronal cells. **A** Representative STED microscopy images of SH-SY5Y cells treated with the indicated $A\beta_{42}$ species at 3.0 µM (monomer equivalents) for 1 h. Red and green fluorescence indicates respectively the cell membranes and the $A\beta_{42}$ species, detected with the indicated Abs. **B** The histograms represent the results of a semi-quantitative analysis of the green fluorescent signal. Experimental errors are S.E.M. ($n = 3$). Samples were analysed by Student *t* test relative to untreated cells (**$P < 0.01$, and ***$P < 0.001$), or to cells treated with the same $A\beta_{42}$ species and detected with DesAb-O (§$P < 0.05$, §§$P < 0.01$, §§§$P < 0.001$). 200–250 cells were analysed per condition

oligomers, at least equal to that of a traditional conformation-sensitive Ab.

We then evaluated whether DesAb-O was also able to prevent the neurotoxic effects evoked by $A\beta_{42}$ aggregates, by analysing their mitochondrial status with the MTT reduction test. $A\beta_{42}$ species (3.0 µM, monomer equivalents) were incubated in the absence or presence of an equimolar concentration of DesAb-O for 1 h, and then these solutions were added to the culture medium of SH-SY5Y cells for 24 h. Our results showed that A + oligomers and ADDLs significantly reduced (by 31 ± 3% and 35 ± 3%, respectively) the mitochondrial activity of SH-SY5Y cells as compared to untreated cells, taken as 100% (Fig. 3E), as previously shown [6, 18, 40, 45, 48]. Both types of fibrils were also found to be significantly toxic, even if to a lesser extent with respect

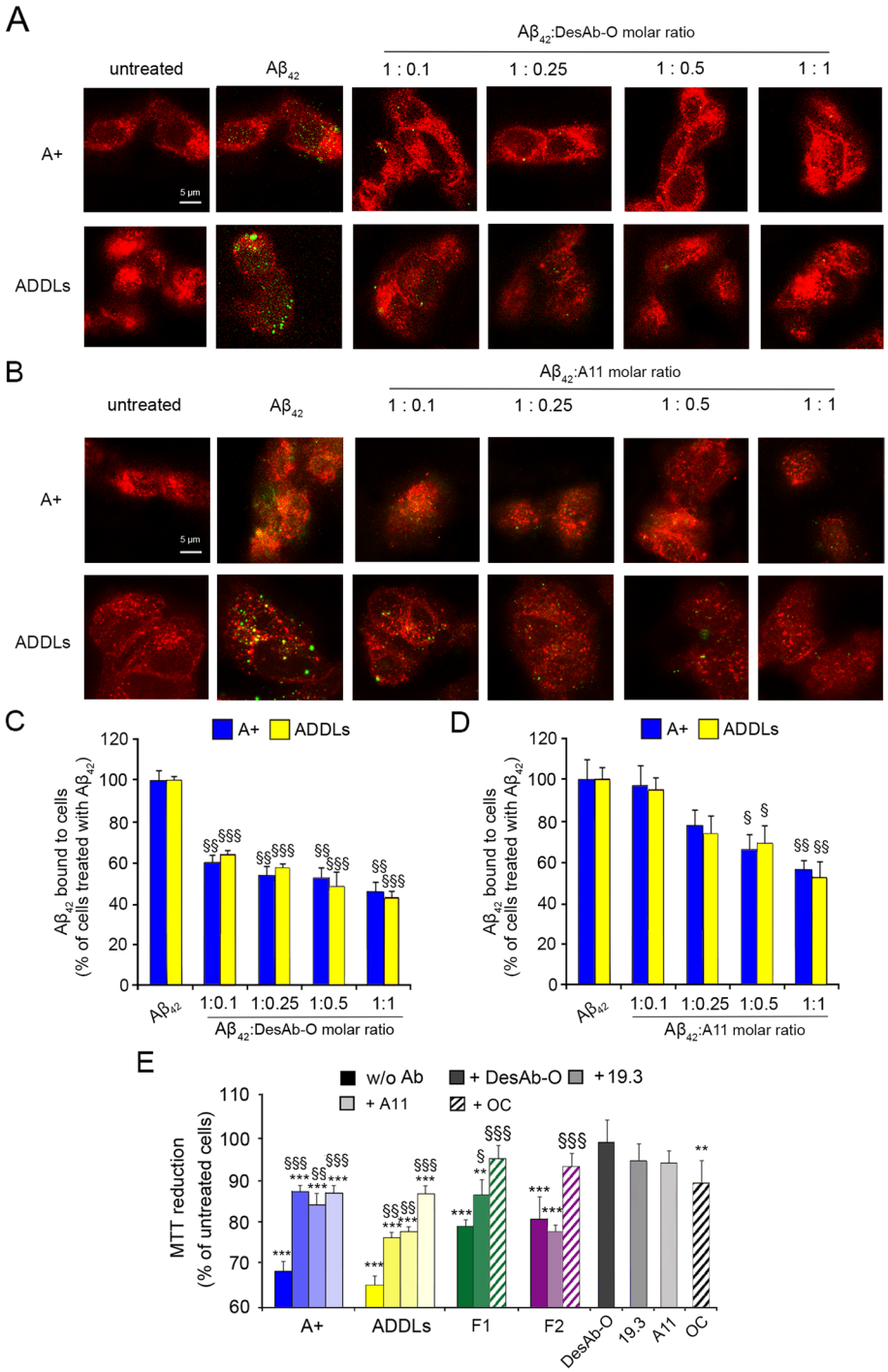

Fig. 3 DesAb-O inhibits the binding of $A\beta_{42}$ oligomers to the neuronal membrane preventing their induced mitochondrial dysfunction. **A**,**B** Representative confocal microscopy images of SH-SY5Y cells treated with 3.0 μM (monomer equivalents) A + oligomers and ADDLs following 1 h pre-incubation in the absence or presence of DesAb-O (**A**) or A11 (**B**) Abs at the indicated $A\beta_{42}$:Abs molar ratios, where molar ratios refer to monomer equivalents. Red and green fluorescence indicates the cell membranes and $A\beta_{42}$ oligomers detected with the 6E10 Ab. **C**,**D** Degree of membrane binding of A + oligomers and ADDLs measured following incubation under the conditions represented in panels A and B, determined as reported in the *Methods* section. **E** MTT reduction in SH-SY5Y cells treated for 24 h with the indicated $A\beta_{42}$ aggregates at a concentration of 3.0 μM (monomer equivalents) following a 1 h pre-incubation in the absence or presence of the indicated Abs. Abs alone were also tested as a control. Experimental errors are S.E.M. ($n = 4$). Samples were analysed by one-way ANOVA followed by Bonferroni's multiple-comparison test relative to untreated cells (*$P < 0.05$, **$P < 0.01$, and ***$P < 0.001$), or to cells treated with the same $A\beta_{42}$ species without any Ab (§$P < 0.05$, §§$P < 0.01$, §§§$P < 0.001$). 200–250 (**A–D**) and 250,000–300,000 (**E**) cells were analysed per condition

to the oligomeric species (the reduction of cell viability was 21 ± 2% and 17 ± 2% for F1 and F2, respectively, as reported in Fig. 3E), confirming previous data [39, 40, 45]. When A + oligomers and ADDLs were pre-incubated for 1 h with DesAb-O, we observed a significant improvement of mitochondrial function (by 18 ± 4% and 11 ± 3%, respectively, with respect to cells treated with the same species in the absence of DesAb-O), whereas the fibril-induced neurotoxicity was not affected by DesAb-O (Fig. 3E), confirming again its high specificity in the targeting of $A\beta_{42}$ oligomeric conformations. The same analysis was performed with the 19.3 and A11 Abs that were found to significantly prevent the cytotoxicity induced by A + oligomers (increase of MTT reduction by 15 ± 5% and 18 ± 4%, respectively) and ADDLs (by 13 ± 3% and 22 ± 3%, respectively), whereas the OC Ab markedly suppressed the cytotoxicity of fibrillar conformations (by 16 ± 4% and 16 ± 5%, respectively), as already shown [45]. Of note, DesAb-O did not affect neuronal viability when added alone to the cell culture medium, thus making it an excellent tool for future tentative therapeutic applications.

DesAb-O detects Aβ42 oligomers in the CSF of AD patients in vitro

Considering the encouraging data obtained with DesAb-O both in vitro and in cultured cells, we then assessed its ability to identify $A\beta_{42}$ species that are present in the CSF of AD patients with respect to the CSF of age-matched control subjects. We performed a series of proof-of-concept experiments on a small set of clinical samples of CSF ($n = 9$ from AD and $n = 4$ from controls) to explore whether our assays could detect differences between the two groups. We first performed a sandwich dot-blot analysis by spotting 2 µl of the capture Abs 6E10 and DesAb-O (corresponding to 0.01 mg/ml and 10 µM, respectively) onto a nitrocellulose membrane that was then incubated with $A\beta_{42}$ species at 2 µM or CSF from AD patients and controls at 0.1 mg/ml. The membranes were then revealed with the 6E10 Ab. This approach, which is different from the classical dot-blot employed in Fig. 1A,B, is useful in a context in which the amount of oligomers we expected to have in the CSF of AD patients was very low. The 6E10 Ab, as expected, showed positive signal with all samples, including the CSFs (Fig. 4A). Despite the improved sensitivity in the recognition of oligomeric species, that gave rise to a high signal (Fig. 4A), DesAb-O was also found to generate a slight cross-reaction with monomers and to a minor extent with fibrils. Interestingly, an intense spot was observed following the incubation of DesAb-O with AD CSFs and only a weak signal with the control CSFs (Fig. 4A).

To further demonstrate the capability of DesAb-O to identify $A\beta_{42}$ oligomers in the CSF of AD patients with respect to control individuals, we performed an indirect sandwich ELISA assay, again to improve specificity and sensitivity. Briefly, we coated the ELISA plate with 1 µM DesAb-O and incubated with decreasing concentrations (4500, 2250, 450, 45, 4.5 and 2.25 pg/ml) of $A\beta_{42}$ species ($A\beta_{42}$ monomer (M), A + oligomers, and F1, the CSFs from AD patients ($n = 9$) and that from control subjects ($n = 4$) at the concentration of 0.25 mg/ml. The plates were then probed with 6E10 as capture Ab. We found that DesAb-O significantly recognised A + oligomers (Fig. 4B, blue bars) down to 2.25 pg/ml with respect to the monomeric and fibrillar forms of $A\beta_{42}$ (Fig. 4B, magenta and green bars, respectively), showing a lower affinity for these forms only at the highest concentration. As a control, we used monomeric αSyn, which was not recognised by DesAb-O, demonstrating again its high specificity for $A\beta_{42}$ (Fig. 4B, orange bar). Notably, DesAb-O generated a high signal with the CSFs of AD patients (Fig. 4B, dark red bar) that appeared significantly different from that obtained with those of control subjects (Fig. 4B, cyan bar).

The ability of DesAb-O to detect $A\beta_{42}$ oligomers in the CSFs of AD patients was also exploited by super-resolution STED microscopy [44]. $A\beta_{42}$ species (25 µM, monomer equivalents) and CSFs from AD patients and controls (0.5 mg/ml) were deposited on a glass coverslip and labelled with 6E10 and DesAb-O Abs. As expected, the 6E10 Ab clearly recognised both preformed A + oligomers and fibrils, even in a 1:1 mixture between oligomeric and fibrillar species (Fig. 4C). In particular, A + oligomers exhibited green fluorescent punctae, which appeared to be small and globular at the very high magnifications allowed by STED microscopy, whereas F1 appeared fibrillar in morphology (Fig. 4C, bottom box magnifications). Monomeric $A\beta_{42}$ is difficult to detect (Fig. 4C), in agreement with the results obtained in a cellular context (Fig. 2A,B). For this reason, the 6E10 Ab did not detect Aβ species in control CSF AD samples, whereas it did with AD CSFs, recognising green fluorescent punctae, globular in shape, some of which apparently larger than oligomeric species (Fig. 4C, bottom box magnifications). In contrast, DesAb-O clearly recognises A + oligomers rather than fibrils, revealing the presence of small globular green fluorescent punctae in the solutions containing the 1:1 mixture (Fig. 4C, bottom box magnifications). We then evaluated the CSFs, observing that DesAb-O can selectively detect small, globular and round species compatible with $A\beta_{42}$ oligomers in the CSFs of AD patients, displaying no signal in the control ones (Fig. 4C, bottom box magnifications).

To validate our experimental approach, we tested another sdAb named DesAb18–24, which has been

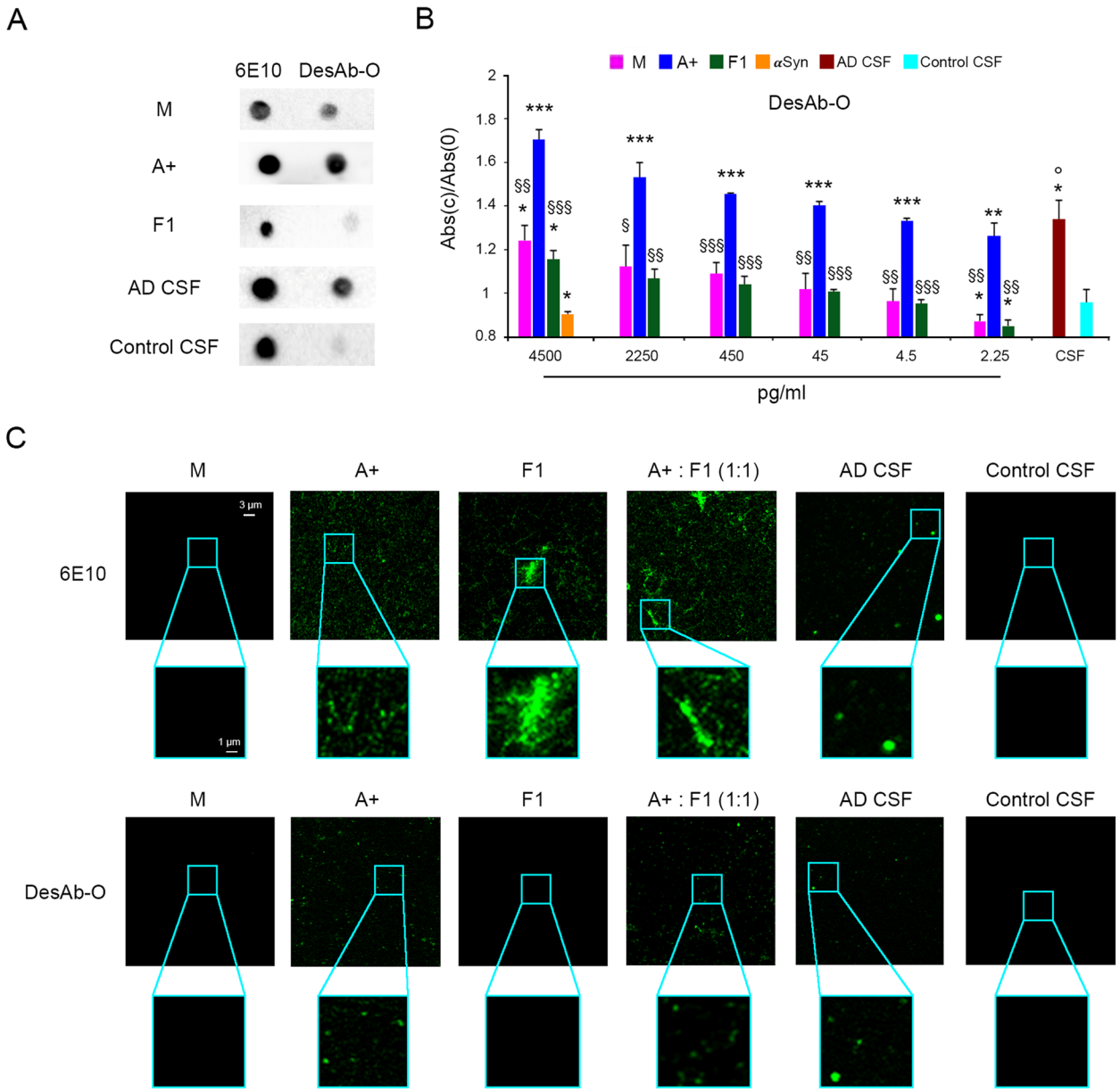

Fig. 4 DesAb-O detects $A\beta_{42}$ oligomers in the CSFs of AD patients in vitro. **A** Representative **s**andwich dot-blot analysis of $A\beta_{42}$ species and CSFs. The capture Abs, 6E10 and DesAb-O were spotted onto nitrocellulose membranes (2 µl corresponding to 0.01 mg/ml and 10 µM). The membranes were incubated with solutions containing different $A\beta_{42}$ species (monomeric $A\beta_{42}$ (M), A + oligomers, fibrils (F1) at 0.01 mg/ml, the CSF from a representative AD patient ($n = 9$) and that from a representative control subject ($n = 4$) at 0.1 mg/ml. Finally, the membranes were probed with the detection 6E10 Ab. **B** Indirect sandwich ELISA. 0.25 mg/ml of CSFs from AD patients and control subjects were adsorbed and quantified by using DesAb-O at 1 µM. Standard curve was obtained with decreasing concentration of $A\beta_{42}$ species formed in vitro. αSyn monomeric protein was used as a negative control. Data were normalised for the corresponding average value at concentration 0 pg/ml. Experimental errors are S.E.M ($n = 4$ for synthetic samples and control CSFs and $n = 9$ for AD CSFs). Samples were analysed by Student *t* test relative to 0 pg/ml (*$P < 0.05$, **$P < 0.01$, ***$P < 0.001$) or to A + (§$P < 0.05$, §§$P < 0.01$, §§§$P < 0.001$) or to control CSF (°$P < 0.05$). **C** Representative STED images showing $A\beta_{42}$ species (M, A +, F1, a mixture containing A + and F1 at 1:1 molar ratio) and CSFs collected from AD patients and controls spotted in a glass coverslip at 25 µM and 0.5 mg/ml, respectively ($n = 4$ for synthetic samples and control CSFs and $n = 9$ for AD CSFs). The green fluorescent signals arise from the staining with 6E10 and DesAb-O Abs. Higher magnifications of the $A\beta_{42}$ species are shown in the boxed areas

rationally designed to target $A\beta_{42}$ fibrils, specifically the region VFFAEDVG [17, 34]. We thus performed an indirect sandwich ELISA assay by coating the wells with 0.5 μM DesAb18–24 and then performing the test as described above. Our results showed that DesAb18–24 clearly recognises $A\beta_{42}$ fibrils down to 4.5 pg/ml, with low affinity for monomeric $A\beta_{42}$ down to 4500 pg/ml and no binding for A + oligomers, except at the highest concentration (Fig. S3A). Notably, DesAb18–24 was found to generate a higher absorbance value from the control CSFs with respect to that observed from AD patients, because of the high cross-reaction with the monomers (Fig. S3B), confirming the difference in terms of total $A\beta_{42}$ between patients and controls reported in literature. The specificity of DesAb18–24 was also evaluated by STED microscopy, showing a clear detection of preformed $A\beta_{42}$ fibrils, without any signal for both CSFs as the monomeric protein is difficult to reveal in this experimental condition (Fig. S3B).

DesAb-O detects $A\beta_{42}$ oligomers present in AD CSFs upon their interaction with neuronal cells

To further evaluate the ability of DesAb-O to target $A\beta_{42}$ oligomers present in the CSFs of AD patients, we applied high-resolution STED microscopy to SH-SY5Y cells exposed to ADDLs, or to the CSFs of AD patients and age-matched control subjects (without pre-incubation with Abs). Following the administration for 5 h of ADDLs at 3.0 μM (monomer equivalents) or CSFs diluted 1:1 with the extracellular medium, the $A\beta_{42}$ aggregates (green channel) were counterstained with DesAb-O or 6E10 Abs and the cell membrane (red channel) with WGA (Fig. 5A,B). Cells exposed to ADDLs exhibited green fluorescent punctae, which appeared to be small and globular at the very high magnifications allowed by STED microscopy (Fig. 5A,B, bottom image magnification). The DesAb-O derived green fluorescent signals were consistent with the results obtained with the 6E10 Ab. In particular, the semi-quantitative analysis revealed that the oligomeric species are localised both intracellularly and extracellularly. Notably, DesAb-O can recognise a number of small and globular intracellular and extracellular $A\beta_{42}$ species in the CSFs of AD patients, with a morphology that resembles that of the oligomeric species (Fig. 5A, bottom image magnification). In addition to the small oligomeric species, the 6E10 Ab can also recognise larger aggregates in the CSFs of AD patients that, at high magnification, appeared round in morphology (Fig. 5B, bottom image magnification). In contrast, cells treated with the CSFs of control subjects and counterstained with both DesAb-O and 6E10 showed the presence of few $A\beta_{42}$ aggregates outside the cells or attached to the membrane, which probably represent nontoxic oligomers that are not able to permeabilise the cell membrane or low amounts of toxic oligomers that do not manifest their toxicity due to their small quantity (Fig. 5AB, bottom image magnification). Similar results were obtained in primary rat cortical neurons exposed to AD and control CSFs and labelled with DesAb-O (Fig. 5C).

DesAb-O prevents neuronal dysfunction induced by the CSFs of AD patients

We finally evaluated whether DesAb-O can also neutralise the cytotoxicity of oligomers present in the CSFs of AD patients. A relatively high volume (ml of sample) is required to perform these experiments, so they were performed on 4 AD and 4 age-matched control CSFs. We first monitored the dysregulation of cytosolic Ca^{2+} homeostasis, which is an early upstream event evoked by extracellular $A\beta_{42}$ oligomers both in cultured neuronal cells and in relevant mouse AD models, where Ca^{2+} ions flow from the extracellular space to the cytosol [7, 43, 54–57]. SH-SY5Y cells were treated for 5 h with the CSFs from AD patients and control subjects diluted 1:1 with the cell culture medium, following or not a 1 h pre-incubation with DesAb-O at 3 μM. The CSFs of AD patients caused a significant influx of Ca^{2+} ions (by 230 ± 11%) relative to untreated cells (Fig. 6A), whereas the CSFs of control subjects generated only a slight and non-significant alteration of Ca^{2+} homeostasis (Fig. 6A). A 1 h pre-incubation with DesAb-O significantly reduced the effect induced by the CSFs of AD patients (by 77 ± 20%), without affecting that observed in cells treated with the control ones (Fig. 6A). As a positive control, 1 μM (monomer equivalents) ADDLs were found to generate an extensive Ca^{2+} influx (by 405 ± 15%, Fig. 6A) that markedly decreased (by 250 ± 26%) following a 1 h pre-incubation with 3 μM DesAb-O. Similar results were obtained in primary rat cortical neurons exposed for 2.5 h to the CSFs of AD patients and control subjects following or not a 1 h pre-incubation with DesAb-O at 3 μM (Fig. 6B). These results confirm the high specificity of DesAb-O in the targeting of neurotoxic $A\beta_{42}$ conformers present in AD CSFs.

The protective effect of DesAb-O was also observed from the analysis of the alteration of membrane permeability induced by $A\beta_{42}$ oligomers, monitoring the release of the fluorescent probe calcein-acetoxymethyl (AM), previously loaded into the cells [48]. SH-SY5Y cells preloaded with calcein-AM were treated with the CSFs of AD patients and controls diluted 1:1 with the extracellular medium for 5 h following or not a 1 h pre-incubation with DesAb-O at 3 μM. Unlike control CSFs, the AD ones caused a significant permeabilisation of the cellular membrane relative to untreated cells, albeit to a lesser extent than ADDLs, used as a positive control (Fig. 6C).

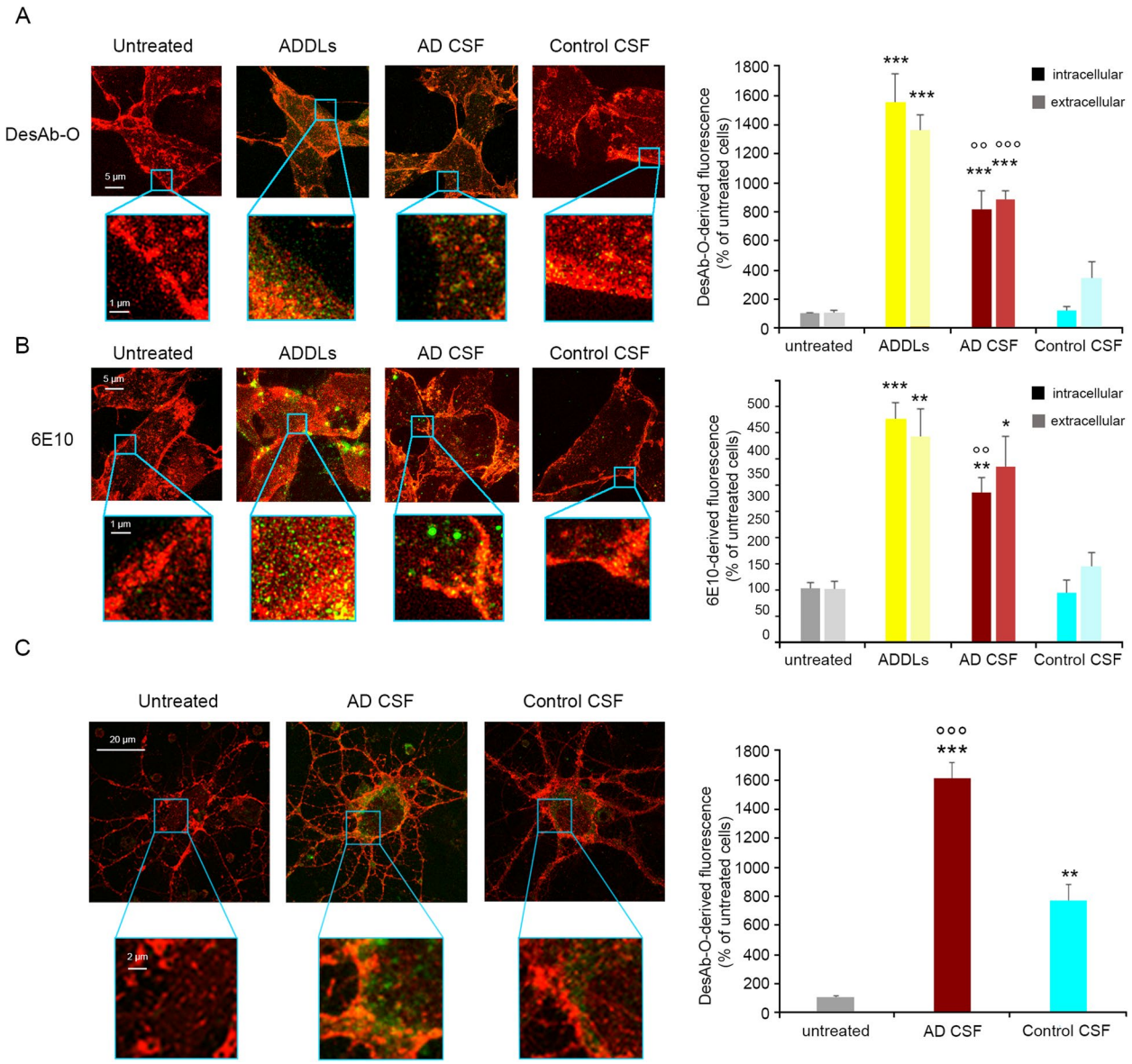

Fig. 5 DesAb-O detects $A\beta_{42}$ oligomers present in the CSFs of AD patients upon their interaction with neuronal cells. **A**,**B** Representative STED microscopy images of SH-SY5Y cells treated with ADDLs at 3.0 µM (monomer equivalents) or CSFs from AD patients and age-matched controls diluted 1:1 with the extracellular medium, for 5 h. Red and green fluorescence indicates the cell membranes and the $A\beta_{42}$ species detected with DesAb-O (**A**) and 6E10 (**B**), respectively. Higher magnifications of the $A\beta_{42}$ species are shown in the boxed areas. The histograms represent the results of a semi-quantitative analysis of the green fluorescent signal. **C** Representative STED microscopy images of primary rat cortical neurons treated with AD and control CSFs, as reported in **A** and **B**. Red and green fluorescence indicates respectively the cell membranes and the $A\beta_{42}$ species detected with DesAb-O. Higher magnifications of the $A\beta_{42}$ species are shown in the boxed areas. Experimental errors are S.E.M. ($n = 4$ for synthetic samples and control CSFs and $n = 9$ for AD CSFs). 200–250 cells were analysed per condition. Samples were analysed by the Student *t* test relative to untreated cells (*$P < 0.05$, **$P < 0.01$ and ***$P < 0.001$), or to cells treated with control CSFs (°°$P < 0.01$ and °°°$P < 0.001$)

Interestingly, DesAb-O significantly prevented the membrane permeabilisation induced by AD CSFs causing an increase of intracellular calcein-derived fluorescence (by 23 ± 9%), although to a minor extent with respect to that observed when pre-incubated with ADDLs (by 41 ± 11%) (Fig. 6C).

We also carried out an MTT reduction test following the administration of CSFs diluted 1:1 with the extracellular medium for 24 h. Unlike the control CSFs, those derived from AD patients caused a modest reduction of the mitochondrial activity of SH-SY5Y cells (by 19 ± 1%) that was reduced by the 1 h pre-incubation with 3 µM

DesAb-O, evident as an improvement of mitochondrial function of 11 ± 2% (Fig. 6D). ADDLs caused a significant reduction of cell viability (by 36 ± 4%) that was prevented by DesAb-O, resulting in an increase of mitochondrial function of 15 ± 7% (Fig. 6D), confirming previous results shown in Fig. 3E.

Overall, these results confirmed the selective ability of DesAb-O to bind and neutralise both in vitro synthesised and patient-derived $A\beta_{42}$ oligomers, representing a promising tool for a future diagnostic, therapeutic and prognostic application in AD.

Discussion

Soluble oligomers of $A\beta_{42}$ have been widely associated with neuronal dysfunction and synaptic loss in AD [5, 13, 14]. Conformational Abs raised by different investigators against independently generated Aβ oligomers have detected these species in AD brains unlike age-matched healthy individuals [18–21]. In the last few years, it has also been demonstrated that Aβ oligomers are present in the CSF of MCI and AD cases, representing a key biomarker candidate [15–17]. Consistent efforts have been made to develop robust assays to characterise and quantify oligomers, discriminating them from the monomeric form [15–17, 58]. In all the ELISA-based methods, a significant overlap in the total mass of Aβ oligomers between patients and controls has been observed, although a small increase in the oligomeric mass has been reported for some cohorts [16, 59]. Recently, highly sensitive biophysical methods have indirectly identified toxic oligomers in the CSF of MCI patients rather than in AD cases, even in a small number of samples [17, 60, 61]. In addition, multiple aggregated forms of $A\beta_{42}$, varying in terms of structure, size, shape and neurotoxicity, have been reported along AD progression [17]. However, due to the lack of suitable sensitive methods, the detection, quantification and isolation of these soluble neurotoxic species from biological fluids remain difficult, because of their heterogeneity, transient nature and very low concentration.

Nanobodies or sdAbs have been recently proposed as promising tools for basic research and potential candidates for diagnostic and therapeutic applications in a range of pathological conditions, thanks to their high target specificity and affinity, as well as low immunogenic potential [33, 62]. In particular, the rational design of sdAbs that selectively target specific Aβ conformers neutralising their neurotoxicity has a great potential of diagnostic and therapeutic value for AD [35, 62–66]. A dozen of sdAbs have shown such potential value for AD in vitro [67], and two of them, namely R3VQ and A2, have reached in vivo imaging as they bind brain Aβ deposits and tau inclusions, respectively [68].

In this work, we examined the possible role of a sdAb, named DesAb-O, targeting a conformational epitope formed by residues 29–36 of $A\beta_{42}$ and exposed by the oligomeric species [35], to selectively detect and neutralise $A\beta_{42}$ oligomers both from synthetic origin and present in AD CSFs. We first characterised its ability to detect a range of pathologically relevant, highly stable and well-characterised $A\beta_{42}$ aggregates (A + and A − oligomers, ADDLs, and two types of fibrils) [38–40], taking advantage of a panel of commercially available conformation-sensitive Abs as controls. The immunoassay analysis revealed a high affinity and selectivity of DesAb-O for $A\beta_{42}$ oligomers, at least equal to that of the A11 and 19.3 Abs, raised against prefibrillar oligomers and ADDLs, respectively [16, 18], with only a minor cross-reaction with the monomeric protein, nontoxic oligomers and fibrillar conformers. We also evaluated the ability of DesAb-O to selectively detect $A\beta_{42}$ oligomers in cultured cells, demonstrating a great performance also in a more physiological condition.

We then revealed that the pre-incubation of DesAb-O with $A\beta_{42}$ oligomers strongly reduces their interaction with neuronal membranes in a dose-dependent manner, and this protective effect appears more evident for DesAb-O than the A11 Ab, at least at low $A\beta_{42}$:Abs molar ratios. This suggests that DesAb-O can detect the

(See figure on next page.)

Fig. 6 DesAb-O prevents neuronal dysfunction induced by the CSFs of AD patients. **A** Intracellular Ca^{2+}-derived fluorescence in SH-SY5Y cells treated for 5 h with ADDLs at 1 μM (monomer equivalents), or with CSFs from AD patients and age-matched control subjects ($n = 4$), diluted 1:1 with the extracellular medium, following 1 h pre-incubation in the absence or presence of DesAb-O at 3 μM. **B** Intracellular Ca^{2+}-derived fluorescence in primary rat cortical neurons treated for 2.5 h with CSFs from AD patients and control subjects ($n = 4$), diluted 1:1 with the extracellular medium, following 1 h pre-incubation in the absence or presence of DesAb-O at 3 μM. **C** Intracellular calcein-derived fluorescence in SH-SY5Y cells treated for 5 h with ADDLs at 1 μM (monomer equivalents), or with CSFs from AD patients and control subjects ($n = 4$), diluted 1:1 with the extracellular medium, following 1 h pre-incubation in the absence or presence of DesAb-O at 3 μM. In all panels, untreated cells are also shown. **D** MTT reduction in SH-SY5Y cells treated for 24 h with ADDLs at 1 μM (monomer equivalents), or with CSFs from AD patients and control subjects ($n = 4$), diluted 1:1 with the extracellular medium, following 1 h pre-incubation in the absence or presence of DesAb-O at 3 μM. Experimental errors are S.E.M. Samples were analysed by Student *t* test relative to untreated cells (*$P < 0.05$, **$P < 0.01$ and ***$P < 0.001$) or to cells treated with samples without DesAb-O (§$P < 0.05$, §§$P < 0.01$ and §§§$P < 0.001$) or to cells treated with control CSFs (°$P < 0.05$ and °°$P < 0.01$). 200–250 (**A**,**C**), 80–150 (**B**) and 250,000–300,000 (**D**) cells were analysed per condition

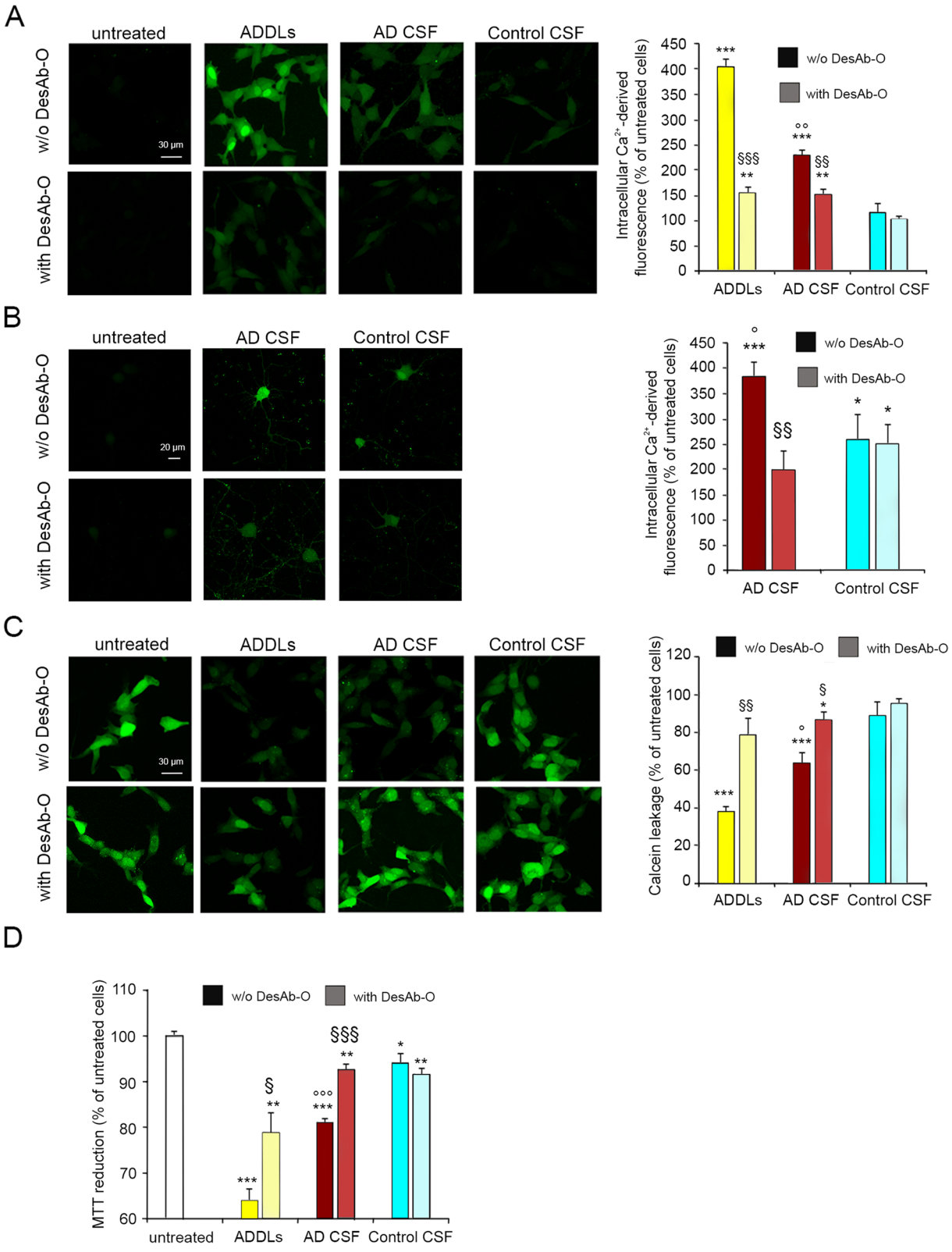

Fig. 6 (See legend on previous page.)

key epitopes normally exposed on the surface of toxic oligomers and responsible for their interaction with the membrane more effectively than the A11 Ab, presumably because of its smaller size, that enables a more precise targeting of critical epitopes. Our results are consistent with those obtained with conformation-sensitive Abs, such as ACU-954 and A-887755, specifically raised against Aβ oligomers, namely ADDLs and globulomers, respectively, that were found to prevent their binding to neurons [21, 69], rescuing the impaired synaptic transmission [21]. The capture of $A\beta_{42}$ oligomers by DesAb-O was also found to prevent their induced mitochondrial dysfunction, in agreement with a large body of evidence supporting the protective effects of Abs, such as A11, OC, AUC-954, A-887755 and PMN310, against neuronal dysfunction [18, 20, 21, 45, 69, 70]. Notably, DesAb-O showed no inherent toxicity when added alone to the cell culture medium, thus making it an excellent tool for future tentative therapeutic applications.

Other sdAbs have been reported to target pathologically relevant $A\beta_{42}$ oligomers. For example, the V31-1 was able to recognise intraneuronal oligomers in human brain slices and to inhibit fibril formation preventing their induced neurotoxicity [64], suggesting a great potential for the detection and diagnosis of Aβ oligomers in AD patients [71]. In addition, two sdAbs, namely PrioAD12 against $A\beta_{40}$ and PrioAD13 against $A\beta_{42}$ [66] can detect Aβ oligomers simultaneously in the blood and retina of APP/PS1 mice before their appearance in the brain, with respect to age-matched wild-type mice controls [72].

When we moved our approach to CSFs, we revealed a remarkable ability of DesAb-O to selectively identify $A\beta_{42}$ oligomers also in a biological fluid from AD patients compared to age-matched control subjects. Previous studies detected $A\beta_{42}$ oligomers in AD CSFs by using two-site ELISA assay and the couple 19.3/82E1 Abs [16], or homotypic ELISA using 82E1 Ab [73] or BAN50 Ab [74]. Even if these reported assays used different oligomer standards, a trend has emerged suggesting that a sub-pg/ml sensitivity is required to detect CSF oligomers [16, 73, 75]. Indeed, in our assay we have been able to measure an average oligomer concentration of c.a. 4.5 pg/ml, in good agreement with previous findings [16, 73, 76]. It is important to clarify that two studies reported a lack of significant change in total aggregates between AD and controls, using both a sdAb, named Nb3, and a mAb, named Bapineuzimab [76, 77]. This suggests that the total amount of the aggregates is not a critical factor in AD CSFs, but it is rather the nature of these aggregates and their effects to be important.

Further analyses were conducted in this work on neuroblastoma cells to test the possible therapeutic potential of DesAb-O against the neurotoxic $A\beta_{42}$ oligomers present in the CSFs of AD patients. We first demonstrated that the CSFs of AD patients caused significant Ca^{2+} influx, membrane permeabilisation and mitochondrial dysfunction, in agreement with previous findings [19, 78–83], and suggesting that the AD CSF contains neurotoxic species. Notably, DesAb-O was found to prevent neuronal dysfunction caused by Aβ oligomers present in the CSFs of AD patients, in agreement with other studies using Nb3 and other Abs against Aβ [79, 80], or extracellular chaperones [82]. It is well known that the shielding of toxic hydrophobic regions exposed on the oligomer surface by either polyclonal or monoclonal Abs, extracellular chaperones and even other proteins present in biological fluids such as transthyretin, appears to be an effective method to suppress the toxicity of misfolded $A\beta_{42}$ oligomers [16, 18, 84, 85], but the high sensitivity and selectivity of DesAb-O and possibly other sdAbs relative to other Abs and chaperones could offer a remarkable potential of these biotechnological tools against AD particularly in its early stages.

While additional studies are required in larger cohorts of AD patients and controls, our data support the idea that sdAbs raised against $A\beta_{42}$ oligomers could represent a new biotech tool for diagnosing AD in the very early stages of pathology. Moreover, our evidence offers the possibility to explore new therapeutic strategies based on sdAbs for AD and other protein misfolding diseases.

Conclusions

In this work, we demonstrate a great ability of a single-domain antibody (sdAb), named DesAb-O, to selectively identify and counteract $A\beta_{42}$ oligomers in a biologically and relevant heterogenous context, such as the cerebrospinal fluid from AD patients with respect to healthy subjects, taking advantage of an array of different techniques such as dot-blot, ELISA immunoassay, super-resolution STED microscopy and in-cell analyses. Taken together, our data indicate a promising method for the improvement of an early diagnosis of AD and for the generation of novel therapeutic approaches based on sdAbs for the treatment of AD and other devastating neurodegenerative conditions.

Abbreviations

A.T.C.C.	American Type Culture Collection
Ab	Antibody
AD	Alzheimer's disease
ADDLs	Amyloid β-derived diffusible ligands
AFM	Atomic force microscopy
APP	Amyloid precursor protein
$A\beta_{42}$	Amyloid beta 42
BSA	Bovine serum albumin
Calcein-AM	Calcein-acetoxymethyl

CSF	Cerebrospinal fluid
CSFs	Cerebrospinal fluid samples
DMEM	Dulbecco's modified Eagle's medium
DMSO	Dimethyl sulfoxide
EDTA	Ethylenediamine tetraacetic acid
ELISA	Enzyme-linked immunosorbent assay
FBS	Fetal bovine serum
FDA	Food and Drug Administration
FITC	Fluorescein isothiocyanate
Fluo-4 AM	Fluo-4 acetoxymethyl
H_2SO_4	Sulfuric acid
HCl	Hydrogen chloride
HEPES	4-(2-Hydroxyethyl) piperazine-1-ethanesulfonic acid
HFIP	Hexafluoro-2-isopropanol
HRP	Horseradish peroxidase
mAb	Monoclonal antibody
MCI	Mild cognitive impairment
MTT	3-(4,5-Dimethylthiazol-2-yl)-2,5-diphenyltetrazolium bromide
NaCl	Sodium chloride
NaOH	Sodium hydroxide
PBS	Phosphate buffered saline
RT	Room temperature
S.D.	Standard deviation
S.E.M	Standard error of the mean
sdAb	Single-domain antibody
STED	Stimulated emission depletion
TBS	Tris buffered saline
Tris	Tris(hydroxymethyl)aminomethane
VHH	Variable heavy domain of heavy chain
WGA	Wheat germ agglutinin
αSyn	α-Synuclein

Supplementary Information

The online version contains supplementary material available at https://doi.org/10.1186/s13195-023-01361-z.

Additional file 1: Figure S1. 6E10 Ab detects all $A\beta_{42}$ species in a dose-dependent manner. Indirect ELISA measurements taken at increasing concentration of $A\beta_{42}$ species using the 6E10 Ab. Data were normalised for the corresponding average value at concentration 0 μM. Experimental errors are S.D. (*n*=3). Samples were analysed by Student *t* test relative to 0 μM (**P*<0.05, ** *P*<0.01 and ****P*<0.001). **Figure S2.** DesAb-O detects $A\beta_{42}$ oligomers bound to the neuronal membrane and internalized into the cytosol.Representative STED microscopy images showing the basal, median, and apical sections of SH-SY5Y cells treated for 1 h with the indicated $A\beta_{42}$ species at 3.0 μM (monomer equivalents) for 1 h. Red and green fluorescence indicates respectively the cell membranes and the $A\beta_{42}$ species, detected with WGA and DesAb-O Ab. **Figure S3.** DesAb18–24 detects $A\beta_{42}$ fibrils and shows a non-specific signal in the CSF samples (A) Indirect sandwich ELISA assay. 0.25 mg/ml of CSF samples from AD patients and control subjects were adsorbed and quantified using DesAb18–24 at 0.5 μM. Standard curve was obtained with decreasing concentration of $A\beta_{42}$ species formed *in vitro*. Data were normalized for the corresponding average value at concentration 0 pg/ml). Experimental errors are S.E.M. (*n*=4). Samples were analysed by Student *t* test relative to 0 pg/ml (* *P*<0.05, ***P*<0.01, *** *P*<0.001) or to F1 (§ *P*<0.05,§§ *P*<0.01, §§§*P*<0.001) or to control CSF (°° *P*<0.01). (B) Representative STED images showing $A\beta_{42}$ species (M, A+ oligomers, F1, and a mixture containing both A+ and F1 at 1:1 molar ratio) and CSFs collected from AD patients and controls (*n*=4) spotted in a glass coverslip at 25 μM and 0.5 mg/ml, respectively. The green fluorescent signals arise from the staining with DesAb18–24.

Authors' contributions

A.B.: investigation, validation, formal analysis, data curation, visualisation, writing—review and editing. L.N.: investigation, formal analysis, data curation, writing—original draft, writing—review and editing. D.M.V.: investigation, writing—review and editing. F.C.: project administration, writing—review and editing, funding acquisition. C.C.: project administration, writing—review and editing, funding acquisition. F.A.A.: conceptualization, methodology, writing—review and editing, supervision, funding acquisition. R.C.: conceptualization, methodology, formal analysis, writing—original draft, writing—review and editing, supervision, project administration, funding acquisition.

Funding

The work was supported by the Airalzh Foundation (Grants for Young Researchers 2020—AGYR 2020, Project SENSITIZER to R.C.), University of Florence (Fondi Ateneo to R.C., C.C. and F.C.), the Regione Toscana (Bando Ricerca Salute 2018, PRAMA project to F.C., C.C. and R.C.), the UK Research and Innovation (Future Leaders Fellowship MR/S033947/1, to F.A.A.) and Alzheimer's Research UK (ARUK-PG2019B-020, to F.A.A.).

Availability of data and materials

The authors confirm that all data needed to evaluate the conclusions of this study are available within the article.

Declarations

Ethics approval and consent to participate

Not applicable.

Consent for publication

Not applicable.

Competing interests

The authors declare no competing interests.

Author details

[1]Department of Experimental and Clinical Biomedical Sciences, Section of Biochemistry, University of Florence, Florence, Italy. [2]Department of Chemistry, Molecular Sciences Research Hub, Imperial College London, London, UK. [3]Institute of Chemical Biology, Molecular Sciences Research Hub, Imperial College London, London, UK.

Received: 4 October 2023 Accepted: 29 November 2023
Published online: 18 January 2024

References

1. Mucke L. Neuroscience: Alzheimer's disease. Nature. 2009;461(7266):895–7.
2. Rajmohan R, Reddy PH. Aβ and phosphorylated tau accumulations cause abnormalities at synapses of Alzheimer's disease neurons. J Alzheimers Dis. 2017;57(4):975–99.
3. Patterson C. World Alzheimer Report. The state of the art of dementia research: new frontiers. Alzheimer's Disease International. 2018;2018:1–48.
4. Kayed R, Sokolov Y, Edmonds B, McIntire TM, Milton SC, Hall JE, Glabe CG. Permeabilization of lipid bilayers is a common conformation-dependent activity of soluble amyloid oligomers in protein misfolding diseases. J Biol Chem. 2004;279(45):46363–6.
5. Benilova I, Karran E, De Strooper B. The toxic Aβ oligomer and Alzheimer's disease: an emperor in need of clothes. Nat Neurosci. 2012;15(3):349–57.
6. Evangelisti E, Cascella R, Becatti M, Marrazza G, Dobson CM, Chiti F, Stefani M, Cecchi C. Binding affinity of amyloid oligomers to cellular membranes is a generic indicator of cellular dysfunction in protein misfolding diseases. Sci Rep. 2016;6:32721.
7. Bigi A, Cascella R, Fani G, Bernacchioni C, Cencetti F, Bruni P, Chiti F, Donati C, Cecchi C. Sphingosine 1-phosphate attenuates neuronal dysfunction induced by Aβ oligomers through endocytic internalization of NMDA receptors. FEBS J. 2023;290(1):112–33.
8. Cline EN, Bicca MA, Viola KL, Klein WL. The Aβ oligomer hypothesis: beginning of the third decade. J Alzheimers Dis. 2018;64(s1):S567–610.
9. Selkoe DJ. Alzheimer disease and aducanumab: adjusting our approach. Nat Rev Neurol. 2019;15(7):365–6.
10. Westerman MA, Cooper-Blacketer D, Mariash A, Kotilinek L, Kawarabayashi T, Younkin LH, Carlson GA, Younkin SG, Ashe KH. The relationship

between Aβ and memory in the Tg2576 mouse model of Alzheimer's disease. J Neurosci. 2002;22(5):1858–67.
11. Selkoe DJ. Cell biology of protein misfolding: the examples of Alzheimer's and Parkinson's diseases. Nat Cell Biol. 2004;6(11):1054–61.
12. Hardy JA, Higgins GA. Alzheimer's disease: the amyloid cascade hypothesis. Science. 1992;256(5054):184–5.
13. Limbocker R, Cremades N, Cascella R, Tessier PM, Vendruscolo M, Chiti F. Characterization of pairs of toxic and nontoxic misfolded protein oligomers elucidates the structural determinants of oligomer toxicity in protein misfolding diseases. Acc Chem Res. 2023;56(12):1395–405.
14. Haass C, Selkoe DJ. Soluble protein oligomers in neurodegeneration: lessons from the Alzheimer's amyloid beta-peptide. Nat Rev Mol Cell Biol. 2007;8(2):101–12.
15. Hefti F, Goure WF, Jerecic J, Iverson KS, Walicke PA, Krafft GA. The case for soluble Aβ oligomers as a drug target in Alzheimer's disease. Trends Pharmacol Sci. 2013;34(5):261–6.
16. Savage MJ, Kalinina J, Wolfe A, Tugusheva K, Korn R, Cash-Mason T, Maxwell JW, Hatcher NG, Haugabook SJ, Wu G, Howell BJ, Renger JJ, Shughrue PJ, McCampbell A. A sensitive Aβ oligomer assay discriminates Alzheimer's and aged control cerebrospinal fluid. J Neurosci. 2014;34(8):2884–97.
17. De S, Whiten DR, Ruggeri FS, Hughes C, Rodrigues M, Sideris DI, Taylor CG, Aprile FA, Muyldermans S, Knowles TPJ, Vendruscolo M, Bryant C, Blennow K, Skoog I, Kern S, Zetterberg H, Klenerman D. Soluble aggregates present in cerebrospinal fluid change in size and mechanism of toxicity during Alzheimer's disease progression. Acta Neuropathol Commun. 2019;7(1):120.
18. Kayed R, Head E, Thompson JL, McIntire TM, Milton SC, Cotman CW, Glabe CG. Common structure of soluble amyloid oligomers implies common mechanism of pathogenesis. Science. 2003;300(5618):486–9.
19. Gong Y, Chang L, Viola KL, Lacor PN, Lambert MP, Finch CE, Krafft GA, Klein WL. Alzheimer's disease-affected brain: presence of oligomeric Aβ ligands (ADDLs) suggests a molecular basis for reversible memory loss. Proc Natl Acad Sci U S A. 2003;100(18):10417–22.
20. Kayed R, Head E, Sarsoza F, Saing T, Cotman CW, Necula M, Margol L, Wu J, Breydo L, Thompson JL, Rasool S, Gurlo T, Butler P, Glabe CG. Fibril specific, conformation dependent antibodies recognize a generic epitope common to amyloid fibrils and fibrillar oligomers that is absent in prefibrillar oligomers. Mol Neurodegener. 2007;2:18.
21. Hillen H, Barghorn S, Striebinger A, Labkovsky B, Müller R, Nimmrich V, Nolte MW, Perez-Cruz C, van der Auwera I, van Leuven F, van Gaalen M, Bespalov AY, Schoemaker H, Sullivan JP, Ebert U. Generation and therapeutic efficacy of highly oligomer-specific beta-amyloid antibodies. J Neurosci. 2010;30(31):10369–79.
22. Hof PR, Giannakopoulos P, Bouras C. The neuropathological changes associated with normal brain aging. Histol Histopathol. 1996;11:1075–88.
23. Perl DP. Neuropathology of Alzheimer's disease. Mt Sinai J Med. 2010;77:32–42.
24. Bateman RJ, Xiong C, Benzinger TL, Fagan AM, Goate A, Fox NC, Marcus DS, Cairns NJ, Xie X, Blazey TM, Holtzman DM, Santacruz A, Buckles V, Oliver A, Moulder K, Aisen PS, Ghetti B, Klunk WE, McDade E, Martins RN, et al. Clinical and biomarker changes in dominantly inherited Alzheimer's disease. N Engl J Med. 2012;367:795–804.
25. Vaz M, Silvestre S. Alzheimer's disease: Recent treatment strategies. Eur J Pharmacol. 2020;887: 173554.
26. Karran E, De Strooper B. The amyloid hypothesis in Alzheimer disease: new insights from new therapeutics. Nat Rev Drug Discov. 2022;21(4):306–18.
27. Sevigny J, Chiao P, Bussière T, Weinreb PH, Williams L, Maier M, Dunstan R, Salloway S, Chen T, Ling Y, et al. The antibody aducanumab reduces Aβ plaques in Alzheimer's disease. Nature. 2016;537(7618):50–6.
28. van Dyck CH, Swanson CJ, Aisen P, Bateman RJ, Chen C, Gee M, Kanekiyo M, Li D, Reyderman L, Cohen S, Froelich L, Katayama S, Sabbagh M, Vellas B, Watson D, Dhadda S, Irizarry M, Kramer LD, Iwatsubo T. Lecanemab in Early Alzheimer's Disease. N Engl J Med. 2023;388(1):9–21.
29. Budd Haeberlein S, Aisen PS, Barkhof F, Chalkias S, Chen T, Cohen S, Dent G, Hansson O, Harrison K, von Hehn C, Iwatsubo T, et al. Two randomized phase 3 studies of aducanumab in early Alzheimer's disease. J Prev Alzheimers Dis. 2022;9(2):197–210.
30. Leisher S, Bohorquez A, Gay M, Garcia V, Jones R, Baldaranov D, Rafii MS. Amyloid-lowering monoclonal antibodies for the treatment of early Alzheimer's disease. CNS Drugs. 2023;37(8):671–7.
31. Ackaert C, Smiejkowska N, Xavier C, Sterckx YGJ, Denies S, Stijlemans B, Elkrim Y, Devoogdt N, Caveliers V, Lahoutte T, Muyldermans S, Breckpot K, Keyaerts M. Immunogenicity risk profile of nanobodies. Front Immunol. 2021;12: 632687.
32. Olzscha H, Schermann SM, Woerner AC, Pinkert S, Hecht MH, Tartaglia GG, Vendruscolo M, Hayer-Hartl M, Hartl FU, Vabulas RM. Amyloid-like aggregates sequester numerous metastable proteins with essential cellular functions. Cell. 2011;144(1):67–78.
33. Muyldermans S. Nanobodies: natural single-domain antibodies. Annu Rev Biochem. 2013;82:775–97.
34. Aprile FA, Sormanni P, Perni M, Arosio P, Linse S, Knowles TPJ, Dobson CM, Vendruscolo M. Selective targeting of primary and secondary nucleation pathways in Aβ42 aggregation using a rational antibody scanning method. Sci Adv. 2017;3(6): e1700488.
35. Aprile FA, Sormanni P, Podpolny M, Chhangur S, Needham LM, Ruggeri FS, Perni M, Limbocker R, Heller GT, Sneideris T, et al. Rational design of a conformation-specific antibody for the quantification of Aβ oligomers. Proc Natl Acad Sci USA. 2020;117:13509–18.
36. Sormanni P, Aprile FA, Vendruscolo M. Rational design of antibodies targeting specific epitopes within intrinsically disordered proteins. Proc Natl Acad Sci U S A. 2015;112(32):9902–7.
37. Sormanni P, Aprile FA, Vendruscolo M. Third generation antibody discovery methods: in silico rational design. Chem Soc Rev. 2018;47(24):9137–57.
38. Lambert MP, Barlow AK, Chromy BA, Edwards C, Freed R, Liosatos M, Morgan TE, Rozovsky I, Trommer B, Viola KL, Wals P, Zhang C, Finch CE, Krafft GA, Klein WL. Diffusible, nonfibrillar ligands derived from Aβ are potent central nervous system neurotoxins. Proc Natl Acad Sci U S A. 1998;95(11):6448–53.
39. Dahlgren KN, Manelli AM, Stine WB Jr, Baker LK, Krafft GA, LaDu MJ. Oligomeric and fibrillar species of Aβ peptides differentially affect neuronal viability. J Biol Chem. 2002;277(35):32046–53.
40. Ladiwala AR, Litt J, Kane RS, Aucoin DS, Smith SO, Ranjan S, Davis J, Van Nostrand WE, Tessier PM. Conformational differences between two Aβ oligomers of similar size and dissimilar toxicity. J Biol Chem. 2012;287(29):24765–73.
41. Bradford MM. A rapid and sensitive method for the quantitation of microgram quantities of protein utilizing the principle of protein-dye binding. Anal Biochem. 1976;72:248–54.
42. Capitini C, Bigi A, Parenti N, Emanuele M, Bianchi N, Cascella R, Cecchi C, Maggi L, Annunziato F, Pavone FS, Calamai M. APP and Bace1: Differential effect of cholesterol enrichment on processing and plasma membrane mobility. iScience. 2023;26(5):106611.
43. Fani G, La Torre CE, Cascella R, Cecchi C, Vendruscolo M, Chiti F. Misfolded protein oligomers induce an increase of intracellular Ca^{2+} causing an escalation of reactive oxidative species. Cell Mol Life Sci. 2022;79(9):500.
44. Cascella R, Chen SW, Bigi A, Camino JD, Xu CK, Dobson CM, Chiti F, Cremades N, Cecchi C. The release of toxic oligomers from α-synuclein fibrils induces dysfunction in neuronal cells. Nat Commun. 202;12(1):1814.
45. Bigi A, Loffredo G, Cascella R, Cecchi C. Targeting pathological amyloid aggregates with conformation-sensitive antibodies. Curr Alzheimer Res. 2020;17(8):722–34.
46. Mosmann T. Rapid colorimetric assay for cellular growth and survival: application to proliferation and cytotoxicity assays. J Immunol Methods. 1983;65(1–2):55–63.
47. Evangelisti E, Zampagni M, Cascella R, Becatti M, Fiorillo C, Caselli A, Bagnoli S, Nacmias B, Cecchi C. Plasma membrane injury depends on bilayer lipid composition in Alzheimer's disease. J Alzheimers Dis. 2014;41(1):289–300.
48. Cascella R, Evangelisti E, Bigi A, Becatti M, Fiorillo C, Stefani M, Chiti F, Cecchi C. Soluble oligomers require a ganglioside to trigger neuronal calcium overload. J Alzheimers Dis. 2017;60(3):923–38.
49. Banchelli M, Cascella R, D'Andrea C, Cabaj L, Osticioli I, Ciofini D, Li MS, Skupień K, de Angelis M, Siano S, Cecchi C, Pini R, La Penna G, Chiti F, Matteini P. Nanoscopic insights into the surface conformation of neurotoxic Aβ oligomers. RSC Adv. 2020;10(37):21907–13.

50. Kim KS, Wen GY, Bancher C, Chen CMJ, Sapienza V, Hong H, Wisniewski HM. Detection and quantification of amyloid β-peptide with two monoclonal antibodies. Neurosci Res Comm. 1990;7:113–22.
51. Baghallab I, Reyes-Ruiz JM, Abulnaja K, Huwait E, Glabe C. Epitomic characterization of the specificity of the anti-amyloid aβ monoclonal antibodies 6e10 and 4g8. J Alzheimers Dis. 2018;66(3):1235–44.
52. Schengrund CL. Lipid rafts: keys to neurodegeneration. Brain Res Bull. 2010;82(1–2):7–17.
53. Evangelisti E, Wright D, Zampagni M, Cascella R, Fiorillo C, Bagnoli S, Relini A, Nichino D, Scartabelli T, Nacmias B, Sorbi S, Cecchi C. Lipid rafts mediate amyloid-induced calcium dyshomeostasis and oxidative stress in Alzheimer's disease. Curr Alzheimer Res. 2013;10(2):143–53.
54. Demuro A, Mina E, Kayed R, Milton SC, Parker I, Glabe CG. Calcium dysregulation and membrane disruption as a ubiquitous neurotoxic mechanism of soluble amyloid oligomers. J Biol Chem. 2005;280:17294–300.
55. Arbel-Ornath M, Hudry E, Boivin JR, Hashimoto T, Takeda S, Kuchibhotla KV, Hou S, Lattarulo CR, Belcher AM, Shakerdge N, et al. Soluble oligomeric amyloid-β induces calcium dyshomeostasis that precedes synapse loss in the living mouse brain. Mol Neurodegener. 2017;12(1):27.
56. Cascella R, Cecchi C. Calcium dyshomeostasis in Alzheimer's disease pathogenesis. Int J Mol Sci. 2021;22:4914.
57. Bigi A, Lombardo E, Cascella R, Cecchi C. The toxicity of protein aggregates: new insights into the mechanisms. Int J Mol Sci. 2023;24(9):7974.
58. Li S, Jin M, Liu L, Dang Y, Ostaszewski BL, Selkoe DJ. Decoding the synaptic dysfunction of bioactive human AD brain soluble Aβ to inspire novel therapeutic avenues for Alzheimer's disease. Acta Neuropathol Commun. 2018;6(1):121.
59. Jekel K, Damian M, Wattmo C, Hausner L, Bullock R, Connelly PJ, Dubois B, Eriksdotter M, Ewers M, Graessel E, et al. Mild cognitive impairment and deficits in instrumental activities of daily living: a systematic review. Alzheimers Res Ther. 2015;7(1):17.
60. Grant MKO, Handoko M, Rozga M, Brinkmalm G, Portelius E, Blennow K, Ashe KH, Zahs KR, Liu P. Human cerebrospinal fluid 6E10-immunoreactive protein species contain amyloid precursor protein fragments. PLoS ONE. 2019;14(2): e0212815.
61. Sideris DI, Danial JSH, Emin D, Ruggeri FS, Xia Z, Zhang YP, Lobanova E, Dakin H, De S, Miller A, Sang JC, et al. Soluble amyloid beta-containing aggregates are present throughout the brain at early stages of Alzheimer's disease. Brain Commun. 2021;3(3):fcab147.
62. Zheng F, Pang Y, Li L, Pang Y, Zhang J, Wang X, Raes G. Applications of nanobodies in brain diseases. Front Immunol. 2022;13: 978513.
63. Zameer A, Kasturirangan S, Emadi S, Nimmagadda SV, Sierks MR. Anti-oligomeric Aβ single-chain variable domain antibody blocks Abeta-induced toxicity against human neuroblastoma cells. J Mol Biol. 2008;384(4):917–28.
64. Lafaye P, Achour I, England P, Duyckaerts C, Rougeon F. Single-domain antibodies recognize selectively small oligomeric forms of Aβ, prevent Aβ -induced neurotoxicity and inhibit fibril formation. Mol Immunol. 2009;46(4):695–704.
65. Kasturirangan S, Li L, Emadi S, Boddapati S, Schulz P, Sierks MR. Nanobody specific for oligomeric Aβ stabilizes nontoxic form. Neurobiol Aging. 2012;33(7):1320–8.
66. David MA, Jones DR, Tayebi M. Potential candidate camelid antibodies for the treatment of protein-misfolding diseases. J Neuroimmunol. 2014;272(1–2):76–85.
67. Bélanger K, Iqbal U, Tanha J, MacKenzie R, Moreno M, Stanimirovic D. Single-domain antibodies as therapeutic and imaging agents for the treatment of cns diseases. Antibodies (Basel). 2019;8(2):27.
68. Li T, Vandesquille M, Koukouli F, Dudeffant C, Youssef I, Lenormand P, Ganneau C, Maskos U, Czech C, Grueninger F, Duyckaerts C, Dhenain M, Bay S, Delatour B, Lafaye P. Camelid single-domain antibodies: A versatile tool for in vivo imaging of extracellular and intracellular brain targets. J Control Release. 2016;243:1–10.
69. Shughrue PJ, Acton PJ, Breese RS, Zhao WQ, Chen-Dodson E, Hepler RW, Wolfe AL, Matthews M, Heidecker GJ, Joyce JG, Villarreal SA, Kinney GG. Anti-ADDL antibodies differentially block oligomer binding to hippocampal neurons. Neurobiol Aging. 2010;31(2):189–202.
70. Gibbs E, Silverman JM, Zhao B, Peng X, Wang J, Wellington CL, Mackenzie IR, Plotkin SS, Kaplan JM, Cashman NR. A rationally designed humanized antibody selective for Aβ oligomers in Alzheimer's disease. Sci Rep. 2019;9(1):9870.
71. Pain C, Dumont J, Dumoulin M. Camelid single-domain antibody fragments: Uses and prospects to investigate protein misfolding and aggregation, and to treat diseases associated with these phenomena. Biochimie. 2015;111:82–106.
72. Habiba U, Descallar J, Kreilaus F, Adhikari UK, Kumar S, Morley JW, Bui BV, Koronyo-Hamaoui M, Tayebi M. Detection of retinal and blood Aβ oligomers with nanobodies. Alzheimers Dement (Amst). 2021;13(1): e12193.
73. Hölttä M, Hansson O, Andreasson U, Hertze J, Minthon L, Nägga K, Andreasen N, Zetterberg H, Blennow K. Evaluating Aβ oligomers in cerebrospinal fluid as a biomarker for Alzheimer's disease. PLoS ONE. 2013;8(6): e66381.
74. Herskovits AZ, Locascio JJ, Peskind ER, Li G, Hyman BT. A Luminex assay detects Aβ oligomers in Alzheimer's disease cerebrospinal fluid. PLoS ONE. 2013;8(7): e67898.
75. Georganopoulou DG, Chang L, Nam JM, Thaxton CS, Mufson EJ, Klein WL, Mirkin CA. Nanoparticle-based detection in cerebral spinal fluid of a soluble pathogenic biomarker for Alzheimer's disease. Proc Natl Acad Sci U S A. 2005;102(7):2273–6.
76. Yang T, O'Malley TT, Kanmert D, Jerecic J, Zieske LR, Zetterberg H, Hyman BT, Walsh DM, Selkoe DJ. A highly sensitive novel immunoassay specifically detects low levels of soluble Aβ oligomers in human cerebrospinal fluid. Alzheimers Res Ther. 2015;7(1):14.
77. Drews A, De S, Flagmeier P, Wirthensohn DC, Chen WH, Whiten DR, Rodrigues M, Vincke C, Muyldermans S, Paterson RW, Slattery CF, Fox NC, Schott JM, Zetterberg H, Dobson CM, Gandhi S, Klenerman D. Inhibiting the Ca^{2+} influx induced by human CSF Cell Rep. 2017;21(11):3310–3316.
78. Näslund J, Haroutunian V, Mohs R, Davis KL, Davies P, Greengard P, Buxbaum JD. Correlation between elevated levels of Aβ -peptide in the brain and cognitive decline. JAMA. 2000;283(12):1571–7.
79. Walsh DM, Klyubin I, Fadeeva JV, Cullen WK, Anwyl R, Wolfe MS, Rowan MJ, Selkoe DJ. Naturally secreted oligomers of Aβ protein potently inhibit hippocampal long-term potentiation in vivo. Nature. 2002;416(6880):535–9.
80. Klyubin I, Betts V, Welzel AT, Blennow K, Zetterberg H, Wallin A, Lemere CA, Cullen WK, Peng Y, Wisniewski T, et al. Aβ protein dimer-containing human CSF disrupts synaptic plasticity: prevention by systemic passive immunization. J Neurosci. 2008;28:4231–7.
81. Demuro A, Parker I, Stutzmann GE. Calcium signaling and amyloid toxicity in Alzheimer disease. J Biol Chem. 2010;285(17):12463–8.
82. Yerbury JJ, Wilson MR. Extracellular chaperones modulate the effects of Alzheimer's patient cerebrospinal fluid on $Aβ_{42}$ toxicity and uptake. Cell Stress Chaperones. 2010;15(1):115–21.
83. Lee SJ, Nam E, Lee HJ, Savelieff MG, Lim MH. Towards an understanding of Aβ oligomers: characterization, toxicity mechanisms, and inhibitors. Chem Soc Rev. 2017;46(2):310–23.
84. Cascella R, Conti S, Tatini F, Evangelisti E, Scartabelli T, Casamenti F, Wilson MR, Chiti F, Cecchi C. Extracellular chaperones prevent $Aβ_{42}$-induced toxicity in rat brains. Biochim Biophys Acta. 2013;1832(8):1217–26.
85. Cascella R, Conti S, Mannini B, Li X, Buxbaum JN, Tiribilli B, Chiti F, Cecchi C. Transthyretin suppresses the toxicity of oligomers formed by misfolded proteins in vitro. Biochim Biophys Acta. 2013;1832(12):2302–14.

Publisher's Note